



**UNESCO-IHE**  
Institute for Water Education



**UNIVERSITY OF  
CHEMISTRY AND TECHNOLOGY  
PRAGUE**

Master's dissertation submitted in partial fulfilment of the requirements for the joint degree of

## International Master of Science in Environmental Technology and Engineering

an Erasmus+: Erasmus Mundus Master Course jointly organized by  
Ghent University, Belgium  
University of Chemical Technology, Prague, Czech Republic  
UNESCO-IHE Institute for Water Education, Delft, the Netherlands

Academic year 2014 – 2015

### *Distribution of Co, Cu and Pb in different Particle-size fractions of Polluted Zambian Wetland Sediments using BCR the Sequential Extraction Procedure*

UNESCO-IHE Institute for Water Education, Delft, the Netherlands

Emmanuel Boateng

Promoter: Ken Irvine

Co-promoter: Peter Kelderman

This thesis was elaborated at UNESCO-IHE Institute for Water Education, Delft, the Netherlands and defended at UNESCO-IHE Institute for Water Education, Delft, the Netherlands within the framework of the European Erasmus Mundus Programme "Erasmus Mundus International Master of Science in Environmental Technology and Engineering " (Course N° 2011-0172)



**Erasmus+**

© 2015 Delft, Emmanuel Boateng, Ghent University, all rights reserved.



UNESCO-IHE  
Institute for Water Education



# **Distribution of Co, Cu and Pb in different Particle-size fractions of Polluted Zambian Wetland Sediments using the BCR Sequential Extraction Procedure**

By: Emmanuel Boateng





# **Distribution of Co, Cu and Pb in different Particle-size fractions of Polluted Zambian Wetland Sediments using the BCR Sequential Extraction Procedure**

Master of Science Thesis

**By: Emmanuel Boateng**

Supervisors

**Prof.K. Irvine, PhD (UNESCO-IHE)**  
**Prof. P. Lens, PhD, MSc (UNESCO-IHE)**

Mentors

**P. Kelderman, PhD, MSc (UNESCO-IHE)**  
**M. M. Nabuyanda, MSc (UNESCO-IHE)**

Examination committee

**Prof.K.Irvine, PhD(UNESCO-IHE)**  
**Prof. P.Lens, PhD, MSc (UNESCO-IHE)**  
**P. Kelderman, PhD, MSc (UNESCO-IHE)**  
**M. M. Nabuyanda, MSc (UNESCO-IHE)**

This research is done for the partial fulfilment of requirements for the Master of Science degree at the UNESCO-IHE Institute for Water Education, Delft, the Netherlands

**Delft**  
**August 2015**



Although the author and UNESCO-IHE Institute for Water Education have made every effort to ensure that the information in this thesis was correct at press time, the author and UNESCO-IHE do not assume and hereby disclaim any liability to any party for any loss, damage, or disruption caused by errors or omissions, whether such errors or omissions result from negligence, accident, or any other cause.

©2015 By: Emmanuel Boateng.  
This work is licensed under a Creative Commons Attribution-NonCommercial 4.0 International License.





# Abstract

Fractions of heavy metals and their distribution in natural wetland sediment grain-size particles (< 63 µm and 63-2000 µm) from the Copperbelt, Zambia were investigated. Generally, metal concentration tends to increase as the grain-sizes get finer. Different particle-size fractions were fractionated for metal distributions in order to understand how same sediments exhibit different distribution of metals at each sampling site. A sequential extraction technique proposed by the European Community Bureau of Reference (BCR) was applied to assess the presence of Cobalt, Copper and Lead in the four fractions (acid-soluble, reducible, oxidizable and residual) in seven sediment samples. The pseudo-total metal content was assessed with the microwave-assisted digestion method. Metal concentrations were assessed using Inductively Coupled Plasma Mass Spectrometry (ICP-MS). The results were validated by the analysis of GBW07404 Standard Reference Material for soils. The results showed good agreement with the certified values. The dominant binding phases for Co, Cu and Mn were exchangeable and the carbonate fraction while Pb in all studied sediments was mainly associated with the Fe/Mn oxides. Iron resided mainly in the residual fraction. The BCR sequential extraction analyses revealed that the extractable metals in the three phases exceeded the residual (microwave-assisted digestion) fraction. Similar distributions of the selected metals were observed in the respective sediment particle-sizes. The relationship between sediment characteristics, metal fractions and total metal concentrations was established using a Pearson correlation matrix. Hierarchical cluster analysis of the total metal content in the whole sediment fraction was used to establish similar characteristics in metallic concentrations between the sampling stations. The cluster analysis revealed three clusters of the sampling stations (group I, II and III) signifying possible identical sources of the metals. The RAC results showed that 8 - 99 %, of Mn, 0.8 - 78 %, of Co, 30 - 55 %, of Cu, 0.03 - 51 % of Pb and 0.05 - 4 % of Fe were exchangeable and carbonate fractions. This is an indication of higher environmental risk to the local environments which could be very detrimental to aquatic living resources. Comparison between pseudo-total metal contents and the Canadian Sediment Quality Guidelines revealed that concentrations of Cu and Pb were higher than the Probable Effect Level in most sampling sites, indicating potential adverse effects on aquatic biota exposed to the sediments.

**Keywords:** BCR sequential extraction, grain-size particles, sediments toxicity, wetland, Zambia



# Acknowledgements

The successful completion of this thesis work is attributed to the extensive support and guidance from my promoter, Prof. Ken Irvine and co-promoter, Dr. Peter Kelderman. Also, I sincerely appreciate the kind support given by Prof. Piet Lens and not forgetting my mentor, Mr. Misery Mulele Nabuyanda for his immense contributions towards the entire research.

I wish to express my profound gratitude to the entire laboratory staff of UNESCO-IHE, Institute for Water Education for their unflinching support with regards to technical assistance given during the laboratory analytical work.



# Table of Contents

<b>Abstract</b>	<b>i</b>
<b>Acknowledgements</b>	<b>iii</b>
<b>List of Figures</b>	<b>viii</b>
<b>List of Tables</b>	<b>ix</b>
<b>Abbreviations</b>	<b>x</b>
<b>List of Symbols</b>	<b>xi</b>
<b>1. Introduction</b>	<b>1</b>
1.1. Heavy metals in wetlands	1
1.2. Statement of the problem	2
1.3. Research objectives	3
1.3.1. Main objective	3
1.3.2. Specific objectives	3
1.4. Research questions	3
<b>2. Literature Review</b>	<b>4</b>
2.1. The fate and transport of metals in sediments	4
2.2. Selected metals in the aquatic environment	4
2.2.1. Cobalt	4
2.2.2. Copper	5
2.2.3. Lead	5
2.3. Factors affecting metal mobility and availability in sediments	5
2.3.1. Influence of particle-size distribution on heavy metal concentration in sediments	6
2.3.2. Role of organic matter on metal distribution in sediment	7
2.3.3. Effect of sediment pH on heavy metal distribution	7
2.3.4. Cation exchange capacity (CEC) and electrical conductivity (EC)	7
2.4. Sequential Extraction	8
2.5. Fractions of metals in sediments	10
2.5.1. Metal partitioning	10
2.5.2. Water-soluble fraction	10
2.5.3. Exchangeable fraction	10
2.5.4. Acid-soluble fraction	10
2.5.5. Reducible fraction	10
2.5.6. Oxidizable fraction	11
2.5.7. Residual fraction	11
<b>3. Materials and Methods</b>	<b>12</b>
3.1. Introduction	12
3.2. Description of the study area	12
3.3. Geological terrain and nature of soils	13
3.4. Copper and cobalt mining firms	13
3.5. Climate	13

3.6.	Sediment sampling	14
3.7.	Laboratory analysis of sediments	15
3.7.1.	Microwave-assisted total digestion	16
3.7.2.	Modified three-step sequential extraction procedure	16
3.7.3.	Heavy metals determination	17
3.7.4.	Quality assurance	17
3.8.	Assessment of potential toxicity of heavy metals in sediment	18
<b>4.</b>	<b>Results</b>	<b>19</b>
4.1.	Results	19
4.1.1.	Physical and chemical properties of the studied sediments	19
4.1.2.	Particle-size distribution of the Zambian polluted wetland sediments	20
4.1.3.	Total metal distribution in different particle-size fractions	22
4.1.4.	Mass balance analysis	25
4.1.5.	Metal fractions in different particle-size fractions of the studied sediments	25
4.1.6.	Assessment of potential toxicity of heavy metals in sediment	30
4.1.7.	Assessment of sediment toxicity using Canadian Sediment Quality Guidelines (SQG)	32
4.1.8.	Pearson correlation coefficient matrix for BCR extracted heavy metal concentrations and sediment physico-chemical characteristics	33
Table 4.5	Pearson correlations for sediment physico-chemical characteristics and BCR extracted selected metal concentrations for whole sediment fraction, sediment fractions < 63 µm, and > 63µm (Laboratory duplicates, <i>n</i> = 2).	35
Table 4.5 (Continuation):	Pearson correlations for sediment physico-chemical characteristics and BCR extracted selected metal concentrations for whole sediment fraction, sediment fractions < 63 µm, and > 63 µm (Laboratory duplicates, <i>n</i> = 2).	36
4.1.9.	Similar characteristics in metallic concentrations in sampling stations	37
4.1.10.	Similar characteristics in metallic concentrations in sampling stations	37
<b>5.</b>	<b>Discussion</b>	<b>38</b>
5.1.	Total metal concentrations, percentage recovery rates and mass balance	38
5.2.	Metal distribution	39
5.2.1.	Exchangeable fraction and fraction bound to carbonate (Acid-soluble, F1)	39
5.2.2.	Fraction bound to iron and manganese oxides (Reducible phase, F2)	40
5.2.3.	Fraction bound to organic matter and sulphides (Oxidizable phase, F3)	40
5.2.4.	Fraction bound to sediment crystalline structure (Residual fraction, F4)	41
5.2.5.	Correlation study	42
5.2.6.	Potential metal mobility assessment	42
5.2.7.	Assessment of potential toxicity using Canadian Sediment Quality Guidelines (SQG)	43
<b>6.</b>	<b>Conclusions and Recommendations</b>	<b>44</b>
6.1.	Conclusions	44
6.2.	Recommendations	44
<b>7.</b>	<b>References</b>	<b>45</b>
<b>8.</b>	<b>Appendices</b>	<b>48</b>
Appendix A	Wet sieving analytical data for particle size determination and the corresponding percentages of sediment particle size fractions	48

Appendix B	: Data related to the measurement of physico-chemical characteristics of the studied sediments.	50
Appendix C	Microwave-assisted digestion analytical data for total metal concentrations in different sediment particle-size distribution	51
Appendix D	Mass balance of total metal concentration in difference sediment particle-size fractions	52
Appendix E	BCR-SEP analytical data for metal fractions in different sediment particle size distribution	54
Appendix F	Risk assessment code of selected metals from Zambian polluted wetland sediments	59

# List of Figures

Figure 2.1	Relationship between metal mobility in the different operationally-defined phases and leachant strength of common chemical reagents used for sequential extraction. Adopted from .....	9
Figure 3.1	The study area and sampling location map.....	12
Figure 4.1	Percentage cumulative logarithmic curve showing grain-size distribution of Kabwe inlet....	21
Figure 4.2	Percentage cumulative logarithmic curve showing grain-size distribution Mufulira outlet...22	
Figure 1.3a	Results of total metal concentration ( $\text{mg kg}^{-1}$ ) in the whole sediment fraction.....	23
Figure 1.3b	Results of total metal concentration ( $\text{mg kg}^{-1}$ ) in sediment fraction $< 63 \mu\text{m}$ size.....	24
Figure 1.3c	Results of total metal concentration ( $\text{mg kg}^{-1}$ ) in sediment fraction $> 63 \mu\text{m}$ size.....	24
Figure 1.4a	Results of BCR sequential extraction partitioning ( $\text{mg kg}^{-1}$ ) and distribution of Co in the sediment samples.....	26
Figure 1.4b	Results of BCR sequential extraction partitioning ( $\text{mg kg}^{-1}$ ) and distribution of Cu in the sediment samples.....	26
Figure 1.4c	Results of BCR sequential extraction partitioning ( $\text{mg kg}^{-1}$ ) and distribution of Pb in the sediment samples.....	27
Figure 1.4d	Results of BCR sequential extraction partitioning ( $\text{mg kg}^{-1}$ ) and distribution of Fe in the sediment samples.....	28
Figure 1.4e	Results of BCR sequential extraction partitioning ( $\text{mg kg}^{-1}$ ) and distribution of Mn in the sediment samples.....	29
Figure 1.5a	Risk Assessment Code for selected metals in whole sediment fraction.....	31
Figure 1.5b	Risk Assessment Code for selected metals in sediment particle size fraction $< 63 \mu\text{m}$ .....	31
Figure 1.5c	Risk Assessment Code for selected metals in sediment particle size fraction $> 63 \mu\text{m}$ .....	32
Figure 4.6	Dendrogram indicating similarity in metallic concentration among the sampling sites.....	37
Figure B.1	Cation exchange capacity (CEC) calibration curves for the selected sediment samples.....	50

# List of Tables

Table 3.1	Location, site description and Geographical Position System (GPS) of the seven sampling stations and their probable source of metal pollution (adopted from Sracek et al., 2012).....	14
Table 3.2	Mean concentration of Pseudo-total metal content ( $\text{mg kg}^{-1}$ , dry weight), standard deviation, percentage recovery (% Rec.) and percentage relative standard deviation (% RSD) of the certified reference material (GBW07404).....	18
Table 3.3	Classification of risk assessment code (RAC)(Wang et al., 2010; Sarkar et al., 2014).....	18
Table 4.1	Physico-chemical characteristics of the sediments (Laboratory replicates, $n = 2$ ) .....	19
Table 4.2	Results of the grain-size analysis of Zambian wetland sediments.....	20
Table 4.3	Results for percentage recovery rates in the respective sediment particle-size fractions .....	25
Table 4.4	Total metal concentrations ( $\text{mg kg}^{-1}$ ) and Canadian sediment quality guidelines values .....	33
Table 4.5	Pearson correlations for sediment physico-chemical characteristics and BCR extracted selected metal concentrations for whole sediment fraction, sediment fractions $< 63 \mu\text{m}$ , and $> 63 \mu\text{m}$ (Laboratory duplicates, $n = 2$ ). .....	35
Table A.1	Results of the grain-size analysis for the studied sediments.....	48
Table C.1	Results of total metals concentrations (mean $\pm$ SD, $\text{mg kg}^{-1}$ ) in the respective sediment fractions (Laboratory replicates, $n = 3$ ) .....	51
Table D.1:	Mass balance of total metal concentrations in three sediment particle-size fractions .....	52
Table E.1	Distribution of cobalt (Co) under the four binding sites in different particle-size fractions...	54
Table E.2	Distribution of copper (Cu) under the four binding sites in different particle size fractions..	55
Table E.3	Distribution of lead (Pb) under the four binding sites in different particle size fractions .....	56
Table E.4	Distribution of iron (Fe) under the four binding sites in different particle size fractions.....	57
Table E.5	Distribution of Manganese (Mn) under the four binding sites in different particle size fractions .....	58
Table F.1	Percentage acid-soluble fraction in total metal concentration, (%) in different particle-size fractions of the studied sediments .....	59

# Abbreviations

- AMD - Acid Mine Drainage
- BCR - European Community Bureau of Reference
- CEC - Cation exchange capacity
- EC - Electrical conductivity
- SEP - Sequential Extraction Procedure
- KI3 - Kabwe Lead Mine Discharge Channel Wetland Inlet Sampling Point 3
- KO1- Kabwe outlet Lead Mine Discharge Channel Wetland Outlet Sampling Point 1
- MI2 - Mufurila Stream TD11 Wetland inlet Sampling Point 2
- MM4 - Mufurila Stream TD11 Wetland midpoint Sampling Point 4
- MO3 - Mufurila Stream TD11 Wetland Outlet Sampling Point 3
- UM2 - Uchi Middle point Sampling Point 2
- UO2 - Uchi South Stream Wetland Outlet Sampling Point 2

# List of Symbols

Co - Cobalt

Cu - Copper

Eh - Redox potential

Fe - Iron

Mn - Manganese

Pb - Lead



# CHAPTER 1

## Introduction

---

### 1.1. Heavy metals in wetlands

Natural wetland ecosystems are essential habitats for wildlife (Alhashemi et al., 2013). Wetlands are inhabited by diverse ecological niches with varied ecological importance (Alhashemi et al., 2013). Aside these functions, natural wetlands, for many decades, have been used extensively as natural filters for wastewater purification as they are deemed to be effective, less expensive and alternative means of treating contaminated surface waters (Bragato et al., 2006; Sekomo et al., 2011).

Using natural wetlands in treating industrial metal-containing wastewater can lead to serious environmental hazards if not efficiently managed, (Sekomo et al., 2011) since the wetlands may eventually become contaminated with different kinds of pollutants including heavy metals. Heavy metals in an aquatic ecosystem mostly accumulate in suspended particles and eventually get incorporated in bottom sediments (Kelderman & Osman, 2007; Cynthia et al., 2011; Sekomo et al., 2011; Idriss & Ahmad, 2013). Sediments serve as both sources and sinks for metals and therefore are important environmental compartment of wetland ecosystems in evaluating levels of heavy metal pollution (Cynthia et al., 2011; Alhashemi et al., 2013; Idriss & Ahmad, 2013). Sediments contaminated with heavy metals pose serious environmental risk due to high toxicity, high persistence and bioaccumulation of metals in aquatic organisms and the potential metal entry into the food chain (Copaja et al., 2014; Sungur et al., 2014).

The ability of sediments to accumulate metals is highly influenced by the sediment grain-size distribution (Maslennikova et al., 2012). Sediment particle-size and the resulting total surface area provide adsorptive surfaces for heavy metals accumulation and subsequent bioavailability (John & Leventhal, 1995). Small particle-sizes allow more metal accumulation due to the larger surface area and therefore serve as the major sources of bioavailable metals (Maslennikova et al., 2012; Idriss & Ahmad, 2013). Although finer sediments contain higher metal concentration than coarser fractions, some metals may have strong affinity for coarser sediment fractions (Singh et al., 1999; Maslennikova et al., 2012; Guagliardi et al., 2013). This emphasizes the importance of analysing heavy metals in whole sediments together with different sediment particle-size fractions when evaluating heavy metal pollution in sediments.

Heavy metals present in sediments exist in different geochemical forms which influence their mobility, bioavailability and toxicity (Copaja et al., 2014). Therefore, evaluation of metal mobility and bioavailability using total metal concentration gives only limited and unreliable assessment of potential

metal toxicity in an aquatic environment (Lin et al., 2003). As opposed to total metal concentrations, determination of different geochemical fractions of metals in different binding forms has been recommended by several researchers as an appropriate alternative in assessing metal mobility, bioavailability and toxicity potential (Tessier et al., 1979; Singh et al., 1999; Lin et al., 2003; Morillo et al., 2004; Alhashemi et al., 2013; Copaja et al., 2014; Sungur et al., 2014). Employing sequential extraction procedures in identifying fractions of metals in sediment helps to properly assess the geochemical processes, bioavailability as well as the potential sources of heavy metals (Sungur et al., 2014).

Different sequential extraction procedures (SEP) have been developed to evaluate metal mobility and bioavailability in sediment (Tessier et al., 1979; Sposito et al., 1982; Silveira et al., 2006). Among the wide range of sequential extraction procedures available in literature, the modified Three Step BCR-SEP recommended by the European Community Bureau of Reference (BCR) has been used to standardize all other procedures and is therefore widely adopted by many researchers (Quevauviller et al., 1997; Fernandez et al., 2004; Guevara-Riba et al., 2004; Morillo et al., 2004; Caplat et al., 2005). The BCR-SEP identifies metals into three different fractions, namely, acid-soluble, reducible and oxidizable. In this present study, this BCR-SEP method has been used to determine metal fractions due to its simplicity, wider usage and the used of reference material to control analytical errors (Copaja et al., 2014; Sungur et al., 2014). Furthermore, if the procedure is strictly followed, the BCR-SEP permits data comparison between different environmental samples (Sutherland et al., 2012).

The current study was conducted on sediments from natural wetlands in Zambia with contamination sources strongly linked to the mining industry, leachates from Cu and Co mine waste piles and metallurgical slag deposits (Sracek et al., 2012). Studies on total metal content and metal fractionation in sediment binding forms within the Copperbelt of Zambia have been conducted by other researchers (Ikenaka et al., 2010; Sracek et al., 2012). However, limited literature exists on metal distribution in various particle-size fractions in Zambian wetland sediments. This study therefore aims to evaluate the distribution of metals in different binding forms and to understand how sediment particle-size fractions influence metals distribution.

## **1.2. Statement of the problem**

Finer sediments are the most important fractions for the study of heavy metal contamination due to their strong association with bioavailable metals (Idriss & Ahmad, 2013; Silva et al., 2014; Copaja et al., 2014). As a result, several heavy metal pollution studies in aquatic sediments have mainly been focused on metal distribution in the < 63  $\mu\text{m}$  particle-size fraction (Guevara-Riba et al., 2004; Morillo et al., 2004; Sracek et al., 2012; Alhashemi et al., 2013; Idriss & Ahmad, 2013; Copaja et al., 2014; Silva et al., 2014). However distribution of metals in both finer and coarser sediment particle-size fractions have also been investigated by several researchers (Lin et al., 2003; Maslennikova et al., 2012; Guagliardi et al., 2013) because the capacity of sediments to accumulate heavy metals is strongly linked with its particle-size distribution (Lin et al., 2003). Therefore sediments exhibit different distribution of metals in the various particle-size fractions as influenced by different binding forms.

However, available literature on metal fractions in wetland sediments within the Copperbelt of Zambia evidently shows that there is no systematic investigation on metal distribution in different particle-size fractions. Sracek et al. (2012) investigated metal fractions in surface water and total sediments sampled from Kafue River while Ikenaka et al. (2010) studied heavy metal contamination in both soils and

sediments in strategic polluted areas in Zambia. Above studies reported high metal pollution within the Copperbelt and its surrounding areas. These high metal loadings within the Copperbelt can create serious environmental problems at slightest change in pH resulting from acid spike (Sracek et al., 2012). However, because these studies did not consider metal distribution in different particle-size fractions, it is difficult to determine if metals are accumulated only in finer sediments or substantial amount is concentrated in the coarser fraction. The mobility and or bioavailability of the metals are equally difficult to determine. Thus, there is the need for further information on metal distribution in various particle-size fractions of wetland sediments from the Copperbelt of Zambia. This will enable appropriate evaluation of metal mobility, bioavailability and toxicity potential in the wetland sediments (Guagliardi et al., 2013).

### **1.3. Research objectives**

Due to paucity of information on heavy metal fractionation in sediment particle-size fractions within the Copperbelt of Zambia, the objectives of the study as part of Mr. Misery Mulele Nabuyanda's PhD research were as follows:

#### **1.3.1. Main objective**

The present study seeks to investigate the binding fractions of selected heavy metals in different particle-size fractions of selected Zambian wetland sediments in order to assess the environmental risk of the metals associated with different particle-size fractions.

#### **1.3.2. Specific objectives**

- I. To analyse the distribution of metal binding forms in different particle-sizes of the wetland sediments.
- II. To determine the potential mobility and toxicity of the metals to the aquatic ecosystem.
- III. To establish the association among heavy metals and physico-chemical characteristics of the wetland sediments.

### **1.4. Research questions**

- I. What effect has particle-size fraction on heavy metal distribution in wetland sediments?
- II. What are the dominant heavy metal binding forms in these wetland sediments?

## CHAPTER 2

# Literature Review

---

### 2.1. The fate and transport of metals in sediments

In an aquatic environment, metals occur as soluble and particulate forms. They are distributed by physico-chemical processes such as adsorption, precipitation, complexation, sedimentation, erosion and diffusion. Metals accumulate in sediment mostly by adsorption and complexation processes with organic materials (Peng et al., 2009). Metals bound to sulfide minerals remain immobile as long as reducing condition persists posing little or no risk to aquatic living resources (John & Leventhal, 1995). Metals also have high affinity for clay minerals, iron and manganese oxyhydroxides (Peng et al., 2009). However, variation in sediment physico-chemical characteristics may cause metals to be remobilized and become bioavailable to aquatic biota.

### 2.2. Selected metals in the aquatic environment

According to Okoro and Fatoki (2012), a heavy metal refers to any metallic chemical element that has a relative high density ( $> 4 \text{ g/cm}^3$ ) and is toxic even at lower concentrations. Heavy metals occur naturally in an ecosystem with wide variation in concentrations and therefore are commonly found in aquatic environments. Metals such as Co, Cu, Cr, Fe, Mn, Ni, Se and Zn are essentially required by aquatic living organisms for life processes such as transportation and metabolic activities while others including As, Cd, Pb and Hg are not only biologically non-essential but also toxic to biological tissues (Puttaiah & Kiran, 2007). Even the presence of essential metals in excessive amounts beyond acceptable threshold levels has the potential to interfere with many beneficial uses of aquatic ecosystems due to their toxicity (Puttaiah & Kiran, 2007; Prasanth et al., 2013).

#### 2.2.1. Cobalt

Cobalt naturally occurs in the environment and it is an essential mineral to living organisms. Presence of cobalt in sediments can be both natural and anthropogenic. Natural sources may include wind-bown dust and forest fires while anthropogenic sources are essentially through fertilizer application, mining and smelting of cobalt-bearing ores (Howe et al., 2006). Cobalt when released into an aquatic environment forms complexes with dissolved organic materials; therefore, its sorption to sediment decreases (Howe et al., 2006). In the absence of organic ligands, Co adsorption on mineral surfaces increases (Krupka & Serne, 2002). Sediment characteristics such as pH, redox potential, humic acids and several other factors affect the

speciation and distribution of cobalt in sediment. Adsorption of cobalt to particulate matter and from water to sediments is directly proportional to pH; hence cobalt concentration increases as pH increases from 5 to 7.5 (Howe et al., 2006). Iron and manganese oxide and clay minerals largely control the adsorption of Co in sediments, with Fe and Mn oxides having higher adsorption capacity on Co than clay minerals (Krupka & Serne, 2002; Howe et al., 2006). Sequential extraction of sediments from Kafue River revealed that, Co is bound to Fe-rich particles in suspension (Sracek et al., 2012). Conversely, Co mineral was also observed to be dominant in the oxidizable fraction in sediments from the Ergene River in Turkey (Sungur et al., 2014).

### **2.2.2. Copper**

Copper is essentially required for synthesis of haemoglobin, proper iron metabolism, and maintenance of blood vessels in humans. However, excessive amount of copper can lead to anaemia, liver and kidney damage (Okoro & Fatoki, 2012). Cu originates from carbonate bearing minerals such as malachite and azurite which have high concentrations of copper. Copper is also mostly present in organic matter and/or sulphides; hence its solubility and mobility are markedly controlled by organic matter mineralization (Caplat et al., 2005). In comparison to other metals, copper has the strongest affinity for organic matter (Callender, 2003). However, Tessier et al. (1979) reported significant amount of Cu bound to Fe and Mn oxides in sediments.

### **2.2.3. Lead**

According to the United State Department of Interior Minerals Management Services (1990), Pb is neither an essential nor beneficial element to living organisms. Toxic effect of lead in humans can cause many diseases including neurological and gastrointestinal dysfunctions (Ikenaka et al., 2010). Day et al. (2003) reported that lead originating from mining tailings is unavailable due to its association with sulphides. However, when introduced into aquatic environments, it readily becomes available because it occurs as secondary minerals such as Fe/Mn-lead oxides. This assertion has been confirmed when Pb was found mainly bound to Fe/Mn oxides in sediments (Sarkar et al., 2014). However, other workers have found considerable amount of Pb in carbonate phase (Moore et al., 2015).

## **2.3. Factors affecting metal mobility and availability in sediments**

Metals in aquatic environments are distributed between solid and liquid phases determined by ligand concentration and metal-bond strengths (John & Leventhal, 1995; Peng et al., 2009). Solid phase metals are mainly partitioned into six different fractions, viz; dissolved, exchangeable, carbonate, Fe/Mn oxide, sulphide, organic and crystalline fractions as indicated by sequential extraction (John & Leventhal, 1995). Variations in limnological factors such as grain-size distribution, organic matter content, cation exchange capacity, sediment pH and other factors strongly influence the partitioning, distribution and bioavailability of metals in sediments. A slight change in these factors results in significant variations in metal distribution. Salinity and temperature also influence metal distribution but to a lesser extent (Peng et al., 2009).

### 2.3.1. Influence of particle-size distribution on heavy metal concentration in sediments

According to Förstner (2004) particle-size distribution controls the ability of suspended particles and sediments to accumulate contaminants and that heavy metal distribution is inversely proportional to particle-size fraction. This strong correlation between particle-size and metal concentrations is attributed to sediment mineralogical composition and particle-size fractions (Horowitz, 1985). Both particle-size fraction and total surface area control heavy metal adsorption, mobility and bioavailability in sediments (Zhao et al., 2010). According to John and Leventhal (1995) small particles allow greater metal adsorption than larger particles due to comparatively larger surface-area-to mass ratios. Horowitz (1985) stated that finer sediments provide active sites for physico-chemical sorption and transportation of contaminants due to their larger surface area and serve as substrates upon which metals accumulate. This assertion has been confirmed by Zhao et al. (2010) who reported higher metal concentrations in smaller particle-size fractions than coarser fractions in road-deposited sediment in Beijing, China. Reduced adsorption in finer sediments is therefore associated with increased metal mobility and bioavailability in interstitial water (Lin et al., 2003). Hence, finer sediments are very important in environmental studies because of their higher capacity to accumulate and remobilize heavy metals than coarser sediment fractions. As a result, fraction < 63 µm has been recommended for heavy metal assessment in sediments for a number of reasons including (i) contaminants mostly accumulate in silt/clay particles, (ii) sediment sieving does not cause changes in metal concentrations and (iii) several heavy metal studies performed on < 63 µm fraction allow comparison of results (Förstner, 2004). Elements such as Co and Cu have been found to have high accumulation in silty-clayey fractions (< 63 µm) than the coarser fractions (Guagliardi et al., 2013). Interestingly, higher accumulation of heavy metals in coarser fractions has also been observed leading to the hypothesis that such accumulation may be due to anthropogenic metal input (Parizanganeh, 2008; Lin et al., 2003). For instance, Lin et al. (2003) showed that higher environmental risk was associated with coarser fractions as with the finer particle-size fractions when potential toxicity of metals in both Ke-Ya River and Ell-Ren River sediments was assessed. They found similar concentrations of metals (Cu, Cr, Pb and Zn) in both the finer and coarser particle-size fractions.

Sediment particle-size distribution can be determined by the use of uniformity and curvature coefficients from a sediment cumulative logarithmic curve. The cumulative logarithmic curve indicates how well sediment grain-sizes are "normally" distributed (Imhansoloeva et al., 2011).

The coefficients are described as follows:

Coefficient of uniformity ( $C_u$ )

$$C_u = \frac{D_{60}}{D_{10}} \quad (1)$$

Coefficient of curvature ( $C_c$ )

$$C_c = \frac{(D_{30})^2}{D_{60} \times D_{10}} \quad (2)$$

When  $C_u$  is greater than 4, the sediment is described as well graded and when the  $C_u$  is less than 4, it is considered to be poorly graded. Therefore for sediment to be described as well graded the value of coefficient of uniformity ( $C_u$ ) has to be greater than 4 and  $C_c$  should be within 1 to 3 (Imhansoloeva et al., 2011).  $D_{10}$  is the effective particle-size which represent diameter for which 10 % of the sample is finer

than D10. D30 is the diameter for which 30 % of the sample is finer than D30 while D 60 is the diameter for which 60 % of the sample is finer than D60 (Imhansoloeva et al., 2011).

### **2.3.2. Role of organic matter on metal distribution in sediment**

Organic matter is one of the principal factors controlling adsorption and transformation of metals in sediments. It contributes significantly to chemical speciation, distribution and bioavailability of heavy metals in aquatic sediments (Shetye et al., 2009). Organic matter and mineral surfaces provides active sites for heavy metals while the degradation of organic matter remobilizes metals bound to it (Wang et al., 2010). The degradation of organic matter is also associated with decreasing redox potential in sediments and release of organic acids to keep sediment pH within the acidic range (Silva et al., 2014). These processes both enhance metal desorption, mobility and bioavailability in aquatic environments. In studying metal fractions in sediments from the Ergene River in Turkey, Sungur et al. (2014) observed strong positive correlation between organic matter and oxidizable, mobile and total fractions of Co, Cu and Pb. These researchers concluded that the strong positive linear relationship indicates that organic matter forms complex structures with the metals and directly controls their mobility in sediments. Wang et al. (2010) also stated that, metal-organic carbon association indicates similar migration characteristics in an aquatic ecosystem.

### **2.3.3. Effect of sediment pH on heavy metal distribution**

According to Förstner (2004), sediment pH is a significant limnological factor that controls the mobilization and distribution of metals in sediments. Metals in sediments form complexes with carbonates, and aluminosilicate adsorb onto oxides of iron and manganese or get incorporated in organic complexes (Wright & Welbourn, 2002; Wang et al., 2010). Metal oxides may be dissolved due to variation in sediment pH. Lower pH causes dissolution of the hydrous oxides and release of metals (Wright & Welbourn, 2002; Kelderman & Osman, 2007). The competition between dissolved ions such as  $\text{SO}_4^{2-}$ ,  $\text{Cl}^-$  and hydrogen ions increases significantly at lower pH for adsorption sites and this phenomenon displaces metals from the oxides and minerals (Wright & Welbourn, 2002; Peng et al., 2009). Organic matter degradation and acid volatile sulphide oxidation usually maintain sediment pH within acidic range causing release of metals from binding sites (Peng et al., 2009). Meanwhile, a slight increase in sediment pH has been observed to favour metal adsorption and precipitation in sediments from Tibiri River Estuary (Silva et al., 2014).

Mobility of individual heavy metals in sediment is limited to specific pH ranges, hence metals tend to be adsorbed at different pH values (John & Leventhal, 1995). As a result, the potential release, mobility and precipitation of metals from sediments may differ significantly (Peng et al., 2009). At pH > 4, copper begins to precipitate from interstitial water and its complete precipitation occurs at pH 6 (Balintova et al., 2012), while Pb is likely to be released from sediment at pH 4 (Peng et al., 2009). A positive linear correlation was observed between sediment pH and the reducible fraction of Co in sediment from the Ergene River (Sungur et al., 2014).

### **2.3.4. Cation exchange capacity (CEC) and electrical conductivity (EC)**

Cation exchange capacity is the ability of particles to adsorb and exchange metals in the environment. According to Nematollahi (2015), CEC is a characteristic property of clay minerals that significantly controls metal distribution, hence a good indicator of metal accumulation in sediments. It can also regulate

metal mobility in sediments (Pam et al., 2013). However, other sediment characteristics such as the amount and type of colloid particles, pH and organic matter content considerably affect cation exchange capacity of sediments (Nematollahi, 2015). CEC classification consists of five levels: very low (< 6 meq/100), low (6-12 meq/100), Moderate (12 - 25 meq/100), high (25-40 meq/100) and very high (>40 meq/100) (Nematollahi, 2015). High CEC is an indication of potential metal adsorption by organic matter, clay particles and carbonate compounds in sediments (Nematollahi, 2015). According to Ololade et al. (2008) higher CEC values of aquatic sediments is an indication of silty/clay and organic matter presence. The adsorption capacity of sediments for contaminants has been reported to correlate (0.81\*\*) positively with CEC (Lin & Chen, 1998) . This assertion has been confirmed by Ma et al. (2010) who stated that, environmental samples with relatively higher CEC (25-40 meq/100) have greater adsorption capacity for cations including toxic heavy metals. Using the batch method in investigating adsorption and desorption of Cu and Pb in paddy soils, Ma et al. (2010) observed that paddy soils with the lowest CEC (7.2 cmol<sub>c</sub>/kg) adsorbed the least concentrations of Cu and Pb in comparison to soils with CEC above 7 cmol<sub>c</sub>/kg . Sediment EC is an indicator of an aquatic saline condition (Nematollahi, 2015). Sediment saline capacity affects metal distribution as lower salinity promotes metal bioavailability (Nematollahi, 2015).

## 2.4. Sequential Extraction

Sediments act as adsorptive sites for heavy metals in an aquatic ecosystem. The similar sediment metal accumulation pathways resulting from both natural and anthropogenic sources complicates the determination of metal origin in sediments (Okoro & Fatoki, 2012). Therefore, identifying metal fractions in sediments by sequential extraction is the only appropriate means of assessing sources of metals in an aquatic environment due to the different potential bioavailability of metals associated with the various binding forms (Jain et al., 2008). Sequential extraction of sediment-bound metals identifies the principal binding phases of metals and provides better understanding of the actual and the potential environmental effect of metals in sediments (Tessier et al., 1979; Okoro & Fatoki, 2012). As sequential extraction involves the use of different reagents in isolating fractions of metals, the extractants are applied in successive order of reactivity that corresponds to the less mobility fractions of the metals (Filgueiras et al., 2002). Several steps may be involved and therefore, the objectives of the extraction procedure and the physical characteristics of the sample concern are crucial factors which determine the choice of the sequential extraction method (Filgueiras et al., 2002).

The success of sequential extraction scheme (SES) depends on a number of factors including i) the chemical properties of the extractant used ii) the efficiency of the extractant and iii) experimental parameter effects (Filgueiras et al., 2002). However, in practice, several other factors such as, the sequence of individual steps, specific 'matrix effects' like eg cross-contamination, pH-buffering steps, re-adsorption and heterogeneity together with physical associations (eg. coatings) of the various solid fractions also affect sequential extraction (Filgueiras et al., 2002; Ure & Davidson, 2002). All these factors have significant effects on SES because extractants used are less specific resulting in extracting species of other phases (Filgueiras et al., 2002). In order to ensure a successful sequential extraction scheme, these factors have to be critically evaluated before a suitable extractant is chosen for a specific extraction. These extractants are commonly classified as unbuffered salts, weak acids, reducing agents; oxidising agents and strong acids (Filgueiras et al., 2002). Figure 2.2 illustrates the schematic reactivity of extractants in relationship to the metal mobility in different phases of the sequential extraction.

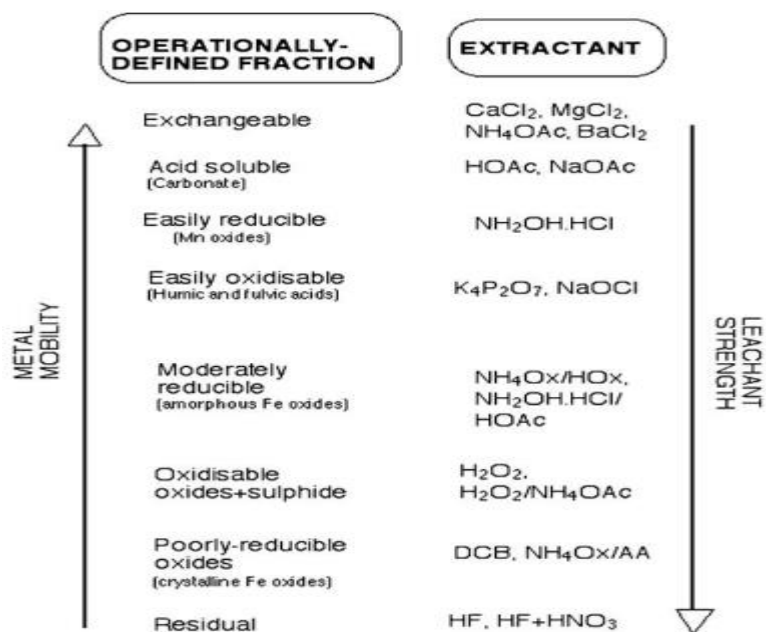


Figure 2.1 Relationship between metal mobility in the different operationally-defined phases and leachant strength of common chemical reagents used for sequential extraction. Adopted from (Filgueiras et al., 2002).

Sequential extraction of heavy metals was originally established by Tessier et al. (1979) as a reliable technique for partitioning metals into various fractions according to their binding forms in soils and sediments. According to these authors, metals can be partitioned into five different fractions, namely exchangeable, carbonate bound, Fe and Mn oxide bound, organic matter and sulphide bound, and residual. These fractions are also referred to as exchangeable, acid-soluble, reducible, oxidizable and residual fractions (Prasanth et al., 2013). However, since sequential extraction is an operationally defined procedure, there have been several modifications made and published by many researchers on the basis that metals are not only fractionated into above five compartments, but are affected by complex chemical processes at and between the metal-sediment interface (Morillo et al., 2004). As a result, literature is now dominated with several sequential extraction procedures with metal partitioning into four (Sposito et al., 1982), six (Kersten & Förstner, 1986) and seven fractions (Silveira et al., 2006). This introduces lack of uniformity in the approach. This lack of homogeneity in the sequential extraction schemes therefore does often not allow intercomparison of results worldwide or validation of procedures (Quevauviller et al., 1997). The European Union's Standards, Measurements and Testing programme (SM & T) therefore adopted a scheme to standardize and harmonize many sequential extraction methods for determination of extractable metal fractions in soils and sediments (Tessier & Campbell, 1987; Quevauviller et al., 1997). This was accompanied with the use of two sediment certified reference materials (BCR- 601 certified for the BCR protocol for soil and BCR-701 certified for metals in sediment) for validation of results to minimize analytic errors (Guevara-Riba et al., 2004). The BCR-SEP as a three-step analytic approach is similar to the original sequential extraction method developed by Tessier et al. (1979) with the exception of combining the "exchangeable" and "carbonate" bound fractions in the first step since these fractions are deemed to the most mobile phases of metals in environmental samples (Wang et al., 2010).

## **2.5. Fractions of metals in sediments**

### **2.5.1. Metal partitioning**

Following sequential extraction procedure, metals in sediments are partitioned into different phases based on their binding forms in sediments. According to Zerbe et al. (1999), the basis of classifying metals in sediments into various chemical forms depends on i) their functions - forms available to aquatic biota ii) operational approach - procedures and extractants used for metal extraction and iii) the oxidation state or specific compounds. As a result, the relative mobility and availability of metals differ significantly among fractions of metals in sediments. Metals therefore partition differently in the individual phases. Metals of anthropogenic origin tend to reside in the preceding fractions while metals found in the residual fraction are mostly of natural origin (Okoro & Fatoki, 2012).

### **2.5.2. Water-soluble fraction**

This phase constitutes the free ions and ions complexed with soluble organic matter and other constituents (Filgueiras et al., 2002). Water-soluble fraction presents the most labile fractions of metals and metalloids in sediments and is the most readily available form for uptake by aquatic biota. According to John and Leventhal (1995), this dissolved fraction consists of carbonate complexes, ion complexes and hydrated ions with their solubility strongly influenced by pH.

### **2.5.3. Exchangeable fraction**

Exchangeable fractions of metals are weakly adsorbed and retained on sediment surfaces by weak electrostatic interaction and may be displaced easily to the water-soluble form (Filgueiras et al., 2002; Ogunfowokan et al., 2013). This phase also constitutes the labile and the most bioavailable forms of metals in sediments (Wang et al., 2010). Exchangeable metals can be released readily into the environment and their remobilization can be caused by changes in ionic composition, influence of adsorption-desorption reactions and acidification (Filgueiras et al., 2002).

### **2.5.4. Acid-soluble fraction**

The acid-soluble fraction constitutes the exchangeable and the carbonate bound phases. Metals in this fraction are adsorbed onto surfaces of carbonate minerals (Filgueiras et al., 2002; Wang et al., 2010). This fraction also presents the most labile forms of metals (exchangeable and other forms) bound to carbonate (Morillo et al., 2004). The carbonate form is a loosely bound phase and liable to changes in environmental conditions (Filgueiras et al., 2002; Morillo et al., 2004). Therefore metals bound to this phase are easily released into the environment upon acid spike.

### **2.5.5. Reducible fraction**

The reducible fraction represents iron and manganese bound metals that may be released upon oxidation of oxides of Fe and Mn compounds (Morillo et al., 2004). The large surface area of amorphous hydrous Fe and Mn oxides enable metals to be highly scavenged by these oxides and hence the reducible phase impacts greatly on metal mobility and bioavailability in aquatic environments (Wang et al., 2010).

### 2.5.6. Oxidizable fraction

Metals bound to organic matter and sulphides constitute the oxidizable fraction and under oxidation conditions, these sediment-bound metals may be released to the environment (Morillo et al., 2004). Metals that form complexes with organic matter are released upon decomposition of organic matter under oxidizing state and at the same time metals bound to sulphides might be extracted during this step (Filgueiras et al., 2002). Organic matter, sulphides and redox potential play important role in metal binding and mobility in sediment (Caplat et al., 2005). Organic substances tend to have high affinity for divalent metallic ions compared to monovalent ions (Okoro & Fatoki, 2012). For example, Caplat et al. (2005) observed the distribution of Pb exhibiting strong affinity for organic matter and sulphides fractions in sediment. Therefore, metal fractions released in the oxidizable step have been reported to have limited mobility because of their association with stable high molecular weight humic substances (Filgueiras et al., 2002). Metals bind to sulphide fraction in sediment according to reaction (3) (Wang et al., 2010):



Sulphide compounds principally control the dissolved metals in aquatic environments hence sediments with high amount of sulphides usually record low metal concentration in their interstitial waters (Wang et al., 2010).

### 2.5.7. Residual fraction

Residual fraction is an essential phase of sequential extraction as it assesses the long term risk of toxic metals (Morillo et al., 2004; Okoro & Fatoki, 2012). This final phase referred to as residual or inert fraction contains metals that are associated with minerals, forming part of the crystalline structure. Iron is bound to the residual fraction in sediment (Caplat et al., 2005). Prasanth et al. (2013) also reported that cadmium and copper mostly resides in residual fraction than organic matter, Fe and Mn and exchangeable fractions. The residual phase is not likely to be released from sediments and therefore considered to be much less toxic to aquatic living organisms (Morillo et al., 2004). However, upon extensive weathering and decomposition processes, metals can become available from the crystalline phase (John & Leventhal, 1995).

## CHAPTER 3

# Materials and Methods

### 3.1. Introduction

This chapter presents the general description of the geographical setting of the study area, geological terrain, climate, collection and preparation of sediment samples as well as the analytical methods adopted in the investigation.

### 3.2. Description of the study area

The study was conducted in the Copperbelt, the Central province of Zambia where intense mining activities had taken place for the past eight decades (Fig. 3.1). Copperbelt is located between latitude  $13^{\circ} 00' 00''$  S and longitude  $28^{\circ} 00' 00''$  E. The region is naturally rich in copper and cobalt and hence it is a historical mining extraction province in Zambia (Liddle et al., 2014). The impacts of these long-time mining activities are expected to leave their imprints on the local environments, especially soils and water bodies.



Figure 3.1 The study area and sampling location map

### 3.3. Geological terrain and nature of soils

The Zambian Copperbelt is generally described to be underlain by rocks of the Kaganga system which is highly enriched with Co and Cu minerals (Křibek et al., 2010; Sracek et al., 2012). According to Sracek et al. (2012) mining occurs principally on the Lower Roan Formation characterised by ore mineralogy such as pyrite ( $\text{FeS}_2$ ), chalcopyrite ( $\text{CuFeS}_2$ ), bornite ( $\text{Cu}_5\text{FeS}_4$ ), chalcocite ( $\text{Cu}_2\text{S}$ ), digenite ( $\text{Cu}_9\text{S}_5$ ), linnaeite ( $\text{Co}_3\text{S}_4$ ), and carrollite. Employing X - ray diffraction analysis, the actual mineralogy of sediment samples taken from Kitwe, Mufulira and Uchi wetlands (tributaries) to the Kafue River were found to contain high amount of hematite ( $\text{Fe}_2\text{O}_3$ ), rutile ( $\text{TiO}_2$ ) and primary silicate minerals such as muscovite (Sracek et al., 2012). In addition, sediments taken from Mufulira tributary contained sulfidic and other silicate minerals (such as amphibole) while Uchi tributary contained primary sulfides such as pyrite, chalcopyrite and bonite. The geology of Kabwe consists of dolomite formation and massive sulphide orebodies containing silicate minerals such as quartz, goethite and hematite (Kamona & Friedrich, 2007). Other secondary minerals such as phosphates, vanadates and carbonates of Zn, Pb, V and Cu can be found within the sulphide ores (Kamona & Friedrich, 2007). However, the sulfidic minerals in sediments from Kitwe were reported to occur in trace amounts and were even not detected in certain portions of the tributary (Sracek et al., 2012). The prevailing soil type in the study area is described as ferralsols (Křibek et al., 2010). Characteristically, ferralsols are acidic soils with pH usually below 5.5 and low exchangeable cations. However, considerable amount of Fe and Al compounds dominate these types of soils.

### 3.4. Copper and cobalt mining firms

Copperbelt being a repository of Cu and Co minerals, virtually all major towns within the region are or used to be centres of mining activities (Fig 3.1). Towns such as Chililabombwe, Chingola, Chambishi, Chibuluma and Mufulira host ore treatment plants and smelters while smelters situated at Kitwe are used for ore refinery (Křibek et al., 2010). As reported by Sracek et al. (2012), Kabwe used to be a very prominent Pb mining town. The lead mines at Kabwe was closed due to lead poisoning (Mulele, personal communication). Many other mining industries in Zambia closed down in the 1980s due to the fall of Cu prices in the world market (Křibek et al., 2010; Liddle et al., 2014). Currently, Kitwe is the centre of Cu mining industries in Zambia while Mufulira host the largest Cu mines on the entire African continent. The extensive Cu and Co smelting activities concentrated within the Copperbelts constitute a major source of heavy metal pollution to the local environments as a result of atmospheric fallout, metal contaminated untreated wastewater discharge and tailings discharge (Sracek et al., 2012).

### 3.5. Climate

The climatic condition of the study area consists of three distinct seasons principally described by Křibek et al. (2010) as Rainy season (November-April), Cold-dry season (May-August) and Hot-dry season (August-October). The mean annual rainfall in the copperbelt varies between 1000-1500 mm. However, Kitwe and Mufulira record an annual rainfall averages of 1320 mm and 1270 mm respectively (Křibek et al., 2010). The occurrence of natural wetlands within the Copperbelt district is attributed to this high and varied annual precipitation (Sracek et al., 2012). The mean temperature of Copperbelt ranges from 9 °C to 23 °C in winter while between 18°C to 23°C is experienced in summer.

### 3.6. Sediment sampling

Sediment samples from three principle historical and present Cu mining towns were used in the study. Sediments were collected from Kabwe, Kitwe and Mufulira (Fig 3.1) from October to December, 2013 by a PhD student (Mr. Misery Mulele Nabuyanda), at UNESCO-IHE, Institute for Water Education. Samples were taken from natural wetlands with possible contamination from a variety of sources including acid mine drainage, discharge of untreated industrial wastewater and leachates from tailings dam deposits, all resulting from the intense Cu mining operations. Each wetland was divided into three sections, namely inlet, middle point and outlet. The sampling points used in this study are part of several sampling points intended for Mr Nabuyanda's PhD research. Details of the sampling locations are presented in Table 3.1. Core sediments were randomly collected from each sampling point using sampling column to different depths varying between 15 cm - 20 cm depending on the depth of the sediments at each particular site. The cores were homogenized and composite samples were placed in food ziploc bags. The ziploc bags and their contents were vacuumed to keep the redox potential at the same level as was in the field. They were then transported to Netherlands and kept in a cold room at 4 °C until analysis.

Table 3.1 Location, site description and Geographical Position System (GPS) of the seven sampling stations and their probable source of metal pollution (adopted from Sracek et al., 2012).

Wetland Location	Site code	Site description	Source of pollution	GPS Position	
Kabwe	KI3	Kabwe inlet sampling point 3	Metal pollution resulting from old lead mining operations (Closed mines).	14°27'16.499" S	28°26'35.215" E
Kabwe	KO1	Kabwe outlet sampling point 1		14°27'38.225" S	28°27'01.1204"E
Mufulira	MI2	Mufulira inlet sampling point 2	Seepage and erosion from old tailings ponds, release of process water from Mufulira mines and smelters	12°33'36.105" S	28°11'38.641" E
Mufulira	MM4	Mufulira midpoint sampling point 4		12°33'55.557" S	28°11'48.089" E
Mufulira	MO3	Mufulira outlet sampling point 3		12°34'02.194" S	28°11'57.888" E
Kitwe/Uchi	UM2	Uchi midpoint sampling point 2	Industrial water discharge from Co and Cu chemical processing plants and washout of fines from large slag deposits		28°13'25.442" E
Kitwe/Uchi	UO2	Uchi outlet sampling point 2		12°50'07.621" S	28°14'12.141" E

## 3.7. Laboratory analysis of sediments

### Analysis of physicochemical properties of the sediments

#### Sediment sample preparation

Samples intended for BCR sequential extraction were prepared by wet sieving method (Adiyiah & Kelderman, 2014). About 60.0 g of the wet sediments was continuously stirred over-night and transferred into a set of standard sieves (0.063 mm and 2 mm) with the larger mesh size on top. The grain-size fractions (silt and clay (< 63 µm) and sand (> 63 µm) were oven dried at 55°C until constant weight was obtained (Guevara-Riba et al., 2004). The fraction > 2 mm was discarded. All the dried sediment fractions (< 63 µm, > 63 µm and the whole sediments) were individually ground into fine powder with clean laboratory mortar and pestle and stored in separate polypropylene containers until analysis. The two particle-size fractions together with the whole sediments were extracted for fractions of metals.

#### Determination of sediment moisture content

Sediment water content was determined after drying approximately 10.0 g of the wet sediments at 105°C for 2.5 hours. The percentage moisture content of the sediment was assessed by the formula below:

$$\% \text{ Moisture content} = \frac{\text{Initial weight} - \text{final weight}}{\text{Initial weight of sediment sample}} \times 100 \quad (4)$$

#### Sediment pH and Conductivity

Sediment pH and conductivity were determined as described by Guevara-Riba et al. (2004). The pH was measured in 1: 2.5 sediment to water ratio using a metrohm 691 pH meter. Twenty-five millilitres of Milli-Q water was added to 10.0 g of each dried sediment fraction in 500 ml beaker. The mixture was stirred for 10 minutes using magnetic stirrer. After allowing the mixture to settle for 30 minutes, pH and conductivity were measured.

#### Grain-size particle analysis

About 50.0 g of the dried sediments was placed in 500 ml de-mineralised water and stirred continuously at 150 rpm over-night using an IKA-WERK top stirrer machine. The homogenized sediment samples were sieved using six Fritsch stainless steel sieves with mesh sizes 2000 µm, 1000 µm, 500 µm, 250 µm, 125 µm and 63 µm. The sieves were placed in succession according to their mesh sizes from the highest to the lowest. After wet sieving, the six fractions ( 2000 µm - 1000 µm, 1000 µm - 500 µm, 500 µm - 250 µm, 250 µm -125 µm, 125 µm - 63 µm and < 63 µm) were dried in an oven at 70°C until a constant weight was obtained (Adiyiah & Kelderman, 2014). The weight of sediments retained on each sieve was determined and a cumulative percentage calculated. Coefficients of uniformity and curvature were assessed to determine grain-size distribution fractions of each sediment sample. There was no laboratory replication because of insufficient samples.

#### Dry weight and Loss-On-Ignition (L.O.I.)

Sediment organic matter content was determined gravimetrically according to Guevara-Riba et al. (2004) as a loss on ignition at 520°C. Three grams of the sediments was dried at 105°C for 2.5 hours. The dried sediments were transferred into a muffled furnace, combusted at 520°C for 3 hours and the loss of weight was determined by the formula below:

## Calculation

$$L.O.I. (Weight \%) = \frac{\text{Sediment weight at } 105^{\circ}\text{C} - \text{Sediment weight at } 520^{\circ}\text{C}}{\text{Sediment weight at } 105^{\circ}\text{C}} \times 100 \quad (5)$$

### Cation exchange capacity (CEC)

The CEC was determined by column percolation method (Kruis, 2007). About 30.0 g subsample of the original sediment was washed with 96 % ethanol and dried at room temperature over-night. Fifty grams of inert silver sand was added to 10.0 g of washed sediment and mixed thoroughly. Seven grams of the inert silver sand was transferred to the bottom of a percolation tube with a glass-wool plugged at the outlet tip. The sediment-sand mixture was transferred to the percolation tube with the aid of a funnel connected to a perforated glass rod to ensure homogeneous packing. An additional 7 grams of inert sand was added at the top. The column was percolated with 250 ml 1 M NaAc (1-2 drops/s) for an hour. Thereafter the column was percolated with 100 ml ethanol for thirty minutes. After discarding the effluent, 100 ml of 1M NH<sub>4</sub>Ac was used to percolate the column for about thirty minutes. The percolate was collected in a 100 ml volumetric flask, filled to the mark with 1 M NH<sub>4</sub>Ac and thoroughly mixed. The preparation was analysed using Atomic Absorption Spectrometry (AAS). The CEC was calculated as follows:

$$CEC \text{ meq Na}/100 \text{ g} = \frac{\text{mg/L (graph)} \times 100}{23 \times 10 \times \text{sample weight (g)}} \times 100 \text{ (dil. factor)} \quad (6)$$

#### 3.7.1. Microwave-assisted total digestion

Sediment samples for total metal determination were oven dried at 55<sup>o</sup>C until constant weight (Guevara-Riba et al., 2004) while the residue from step 4 was oven dried at 105<sup>o</sup>C over-night. The total metal content was determined by closed vessel microwave-assisted digestion (Adiyiah & Kelderman, 2014; Kruis, 2007). About 0.5 g of the oven dried total sediment and the residue were weighed separately into Teflon microwaven tubes. Ten millitres of 65 % concentrated HNO<sub>3</sub> was then added. The microwave destruction lasted for 1 h (20 minutes destruction, 40 mintues cooling) starting at 175<sup>o</sup>C. After destruction, the contents were transferred into 25 ml volumetric flasks and made up to the mark with Mili-Q water. After transferring into 40 ml plastic sampling cups the contents were left over-night to settle.

#### 3.7.2. Modified three-step sequential extraction procedure

The extraction procedure followed the modified version of the initial BCR-SEP (Quevauviller et al., 1997; Guevara-Riba et al., 2004).

**Step 1 (Acid-soluble phase):** This phase was obtained by adding 40 ml of 0.11 mol/L acetic acid to 1.0 g of sediment in a 100-ml borosilicate glass centrifuge tube and covered with laboratory parafilm paper to prevent spillage. The tubes were shaken on 'end-over-end' shaker at 150 rpm for 16 hours at room temperature. The aim of this process was to maintain the samples continuously in suspension during the extraction steps. The extract was separated from the solid residue by centrifugation at 3000 g for 20 min and the supernatant was decanted into a polyethylene container, acidified (to pH < 2) and stored at 4<sup>o</sup>C until analysis. The residue was washed with 20 ml of Mili-Q water. After shaken for 15 minutes, the residue was separated from the supernatant by centrifuging at 3000 g per 20 minutes. The supernatant was carefully decanted and discarded.

**Step 2 (Reducible phase):** This phase was determined by adding 40 ml of 0.5 mol/L hydroxylamine hydrochloride, acid stabilised with 2 mol/L HNO<sub>3</sub> to pH 1.5 and added to the residue from step 1 in the centrifuge tube. The extraction and washing of the residue were performed as in step 1.

**Step 3 (Oxidizable phase):** This phase was removed with 10 ml of 8.8 mol/L hydrogen peroxide (acid-stabilised to pH 2-3) added carefully to the residue from the second step. It was done in small aliquots to avoid losses due to the possible violent reaction of the residue in the centrifuge tube. The tubes were covered loosely with a laboratory parafilm paper and digestion proceeded for 1 h at room temperature with occasional manual shaking. The covered tube was heated for 1 h at 85 °C in a water bath. After, the volume was reduced to a few millilitres by further heating of the uncovered tube. A further aliquot of 10 ml of hydrogen peroxide was added to the residue. The tubes were covered again and heated at 85°C for 1 h. After cooling, 50 ml of 1.0 mol/L ammonium acetate (adjusted to pH 2 ± 1 with nitric acid) was added to the residue and the tubes were then shaken on an ‘end-over-end’ shaker for 16 h (over-night) at room temperature. The remaining operations for separation of the extract were performed as above.

**Step 4 (Residual Phase):** The total metal content in the residue after extraction was determined by Microwave-assisted digestion. The results obtained from the original samples (ie samples not subjected to BCR-SEP) were compared with the sum of the extracted metals from the three steps plus residual ( $\Sigma$  3steps + microwave-assisted extractable from the residue).

### 3.7.3. Heavy metals determination

The analysis of the metals in the supernatant solution following sample digestion and sequential extraction was done using inductively coupled plasma - mass spectrometry (ICP-MS). In addition to Co, Cu and Pb, Fe and Mn contents in the sediment were determined. In literature, these elements are not considered as heavy metals but have been designated as binding sites in this study since their oxide and hydroxide forms (Fe-Mn oxides) have the capacity to scavenge and mobilize metals in sediments upon changes in environment factors such as redox potential and sediment pH (Tessier et al., 1979).

### 3.7.4. Quality assurance

All necessary precautionary measures were adhered to in order to avoid contamination during drying, sieving and storage. Laboratory glass and plastic wares used for the analysis were first cleaned with de-mineralised water, then with 10 % HNO<sub>3</sub> (over-night) and then rinsed with de-mineralised water. All solutions and dilutions were prepared with Mili-Q water. Intermediate standards and reagent solutions were stored in glass bottles to avoid possible contamination from plastic. The precision of the extraction was evaluated by laboratory replicates (n = 2) for each extraction step and laboratory replicates (n = 3) for total metal determination. Certified Reference Material (GBW07404) for soil was used to validate the extraction steps because the recommended Certified Reference Materials BCR-701 and 601 were unavailable. During the digestion of the sediments, method blanks (65 % concentrated HNO<sub>3</sub>) were included in each set of samples digested for the total metal determination. For the three extraction steps, the blanks included were the respective reagent(s) recommended for each step without sediment samples. Mass balance of the BCR-SEP was established by comparing the sum of the products of heavy metal concentrations in each fraction to the heavy metal concentrations in the original sediments. The recovery of the sequential extraction procedure was evaluated as follows:

$$\% \text{ Recovery} = [(step1 + step2 + step3 + Residual)/total] \times 100 \quad (7)$$

The percentage relative standard deviations show that the obtained values are in good agreement with the certified values recording percentage recovery above 95 % for all the extracted metals. Therefore, the obtained results for both total metal content and the amounts of extractable metals following BCR-SEP validate the applied procedures (Table 3.2). Generally, the percentage difference between laboratory duplicates ranged from 0.1 % to 4 % with an average of 1.4 %.

Table 3.2 Mean concentration of Pseudo-total metal content (mg kg<sup>-1</sup>, dry weight), standard deviation, percentage recovery (% Rec.) and percentage relative standard deviation (% RSD) of the certified reference material (GBW07404)

Element	Certified	Determined	% Rec.	% RSD
Co	22 ± 2	21.3± 0.6	96.7	2.72
Cu	40 ± 3	38.2 ± 0.5	95.6	1.28
Pb	58 ± 5	62.3 ± 0.6	107	0.92
Fe	-	65000 ± 219.2	-	0.34
Mn	1420 ± 75	1400 ± 0.7	97.5	0.05

Results expressed as three parallel sample determinations (Laboratory replicates)

Additionally, mass balance for the total metal concentrations in the particle-size fractions in comparison to that in the whole sediments was evaluated following the equation below:

$$\% \text{ Mass balance} = (\% \text{ Finer} * \text{mg/kgHM in } < 63 \mu\text{m}) + (\% \text{ sand} * \text{mg/kg HM in } > 63 \mu\text{m}) \times 100 \quad (8)$$

### 3.8. Assessment of potential toxicity of heavy metals in sediment

The risk assessment code (RAC) was used in assessing the potential toxicity and bioavailability of metals in the wetland sediments (Wang et al., 2010; Sarkar et al., 2014; Sungur et al., 2014). The RAC mainly considers the sum of the exchangeable and carbonate fractions in assessing the availability of selected metals in soil/sediments. However, in the case of BCR-SEP, these fractions are combined in the acid soluble phase. According to RAC guidelines, a soil or sediment will be considered safe for the environment if any metal in that environmental sample releases in exchangeable and carbonates fractions, less than 1 % of the total metal concentration. However, if a sediment with 11-30 % exchangeable and carbonates fractions will pose a medium risk to the environment. Sediments releasing exchangeable and carbonate fractions of any metal above 50 % of the total metal is considered highly risky to the environment (Sarkar et al., 2014). Table 3.2 gives the details of criteria for RAC.

Table 3.3 Classification of risk assessment code (RAC)(Wang et al., 2010; Sarkar et al., 2014)

Grade	Exchangeable and bound to carbonate metal (%)	Risk
I	< 1	No risk
II	1 - 10	Low risk
III	11 - 30	Medium risk
IV	31 - 50	High risk
V	> 50	Very high risk

## CHAPTER 4

# Results

### 4.1. Results

This chapter presents the physico-chemical characteristics and the heavy metal contamination by cobalt, copper, and lead in the wetland sediments.

#### 4.1.1. Physical and chemical properties of the studied sediments

The physico-chemical characteristics of the studied sediment samples are presented in Table 4.1. The results show that moisture content ranged from 19.8 % for Kabwe inlet (KI3) to 37.9 % for Mufulira outlet (MO3). The pH values for Mufurila inlet (MI2), Uchi midpoint (UM2) and outlet (UO3) were found to be neutral, viz 7.0-7.2 respectively. Other sampling sites had pH values ranging between 6.4 - 6.9, indicating that the sediments were slightly acidic to neutral. The temperature at which the EC was measured ranged between 21.4 - 22.5 °C for all sampling sites. The sediment percentage organic matter contents (% DW) were between 26.0 at MI2 and 3.5 at UO2. KO1, MM4 and KI3 had about equal CEC values (Table 4.1). The relatively high EC (3700  $\mu\text{S}/\text{cm}$ ) was recorded in sediments from Kwabwe outlet (KO1) while Mufulira midpoint (MM4) had the least EC (580  $\mu\text{S}/\text{cm}$ ). Appendix B gives the CEC calibration curve for the selected sediments.

Table 4.1 Physico-chemical characteristics of the sediments (Laboratory replicates, n = 2)

Sampling station	Moisture content 105 <sup>0</sup> C (%)	Temperature (°C)	pH (H <sub>2</sub> O) 1:2.5	Loss on Ignition 520 <sup>0</sup> C (%)	CEC meq Na/100 g	Electrical Conductivity (EC) $\mu\text{S}/\text{cm}$
KI3	19.8	21.4	6.9	17.8	15.3	1100
KOI	25.9	21.6	6.4	11.6	17.1	3700
MI2	36.7	21.5	7.0	26.0	12.0	2200
MM4	34.4	22.2	6.9	6.3	16.8	580
MO3	37.9	21.6	6.7	5.3	13.3	1200
UM2	20.8	21.6	7.1	7.1	3.4	1200
UO2	25.5	22.5	7.2	3.5	7.3	1100

#### 4.1.2. Particle-size distribution of the Zambian polluted wetland sediments

Grain-size distribution in the studied sediments revealed small to medium variation in the wetland sediments. Results indicate that pebble fraction of the sediments ranged from 0.0 % to 4.5% (Appendix A). This fraction was not used in further calculation because it is not considered as sediment (Kruis, 2007). The highest silty/clay (< 0.063 mm) fraction was recorded at KO1 (68%) and the least at UM2 (28 %) (Table 4.2). The very fine sand (0.125 - 0.063 mm) and the silty/clay (< 0.063 mm) were the dominant fractions in the sediment samples from all the sampling sites which ranged from (10 % to 34 %) and (28 % to 68 %) respectively (Appendix A). Other particle-size fractions were very coarse sand (2.0 - 1.0 mm), coarse sand (1.0 - 0.5 mm), medium sand (0.50 - 0.25 mm) and fine sand (0.25 - 0.125 mm). The dominance of the above remaining fractions ranged from (0.2 % to 7 %) for very coarse sand, (0.7 % to 7 %) for coarse sand, (2 % to 11 %) for medium sand, and (7 % to 34 %) for fine sand (Appendix A).

Table 4.2 Results of the grain-size analysis of Zambian wetland sediments

Site	Particle-size				Coefficient		Sand (%)	Finer (%)	Classification (Unified)
	D <sub>10</sub> (mm)	D <sub>30</sub> (mm)	D <sub>50</sub> (mm)	D <sub>60</sub> (mm)	C <sub>u</sub>	C <sub>c</sub>			
KI3	0.06	0.078	0.11	0.15	2.50	0.68	43	57	SP*
KO1	0.07	0.081	0.10	0.11	1.57	0.85	32	68	SP*
MI2	0.07	0.092	0.14	0.16	2.25	0.75	48	52	SP*
MM4	0.08	0.110	0.18	0.27	3.60	0.60	61	39	SP*
MO3	0.06	0.095	0.13	0.17	2.83	0.88	49	51	SP*
UM2	0.08	0.140	0.22	0.28	3.5	0.88	72	28	SP*
UO2	0.065	0.120	0.17	0.19	2.92	1.17	60	40	SP*

C<sub>c</sub>= Coefficient of curvature, C<sub>u</sub> = Coefficient of uniformity, \*SP = poorly graded

Using the Unified Soil Classification System (USCS) the graduation coefficients such as uniformity and curvature were used to determine the sortedness of the sediment grain-size distribution with the aid of the percentage cumulative logarithmic curves (Fig. 4.1 and Fig. 4.2). The results show that all the sediment samples from the studied sites are poorly graded, suggesting homogenous particle size distribution (Table: 4.2). Meanwhile, the average (D<sub>50</sub>) sediment grain-size distribution which represents equal distribution of finer and coarser fractions at the various sampling locations follows the order (mm): UM2 (0.22) > MM4 (0.18) > UO2 (0.17) > MO3 (0.13) > KI3 (0.11) > KO1 (0.10) (Table: 4.2).

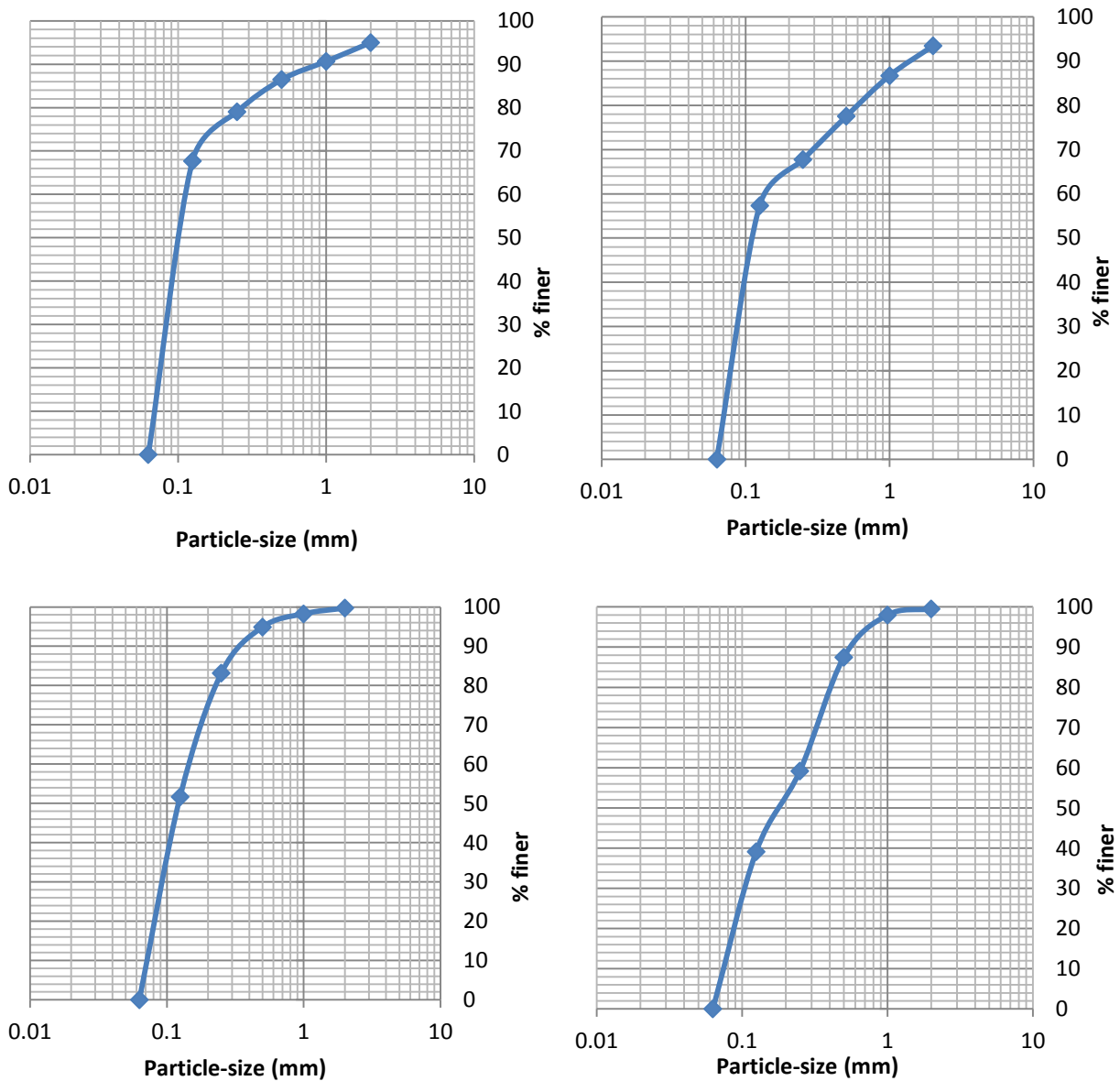


Figure 4.1 Percentage cumulative logarithmic curve showing grain-size distribution of Kabwe inlet (Top left) and Kabwe outlet (Top right), Mufulira inlet (bottom left) and Mufulira midpoint (bottom right)

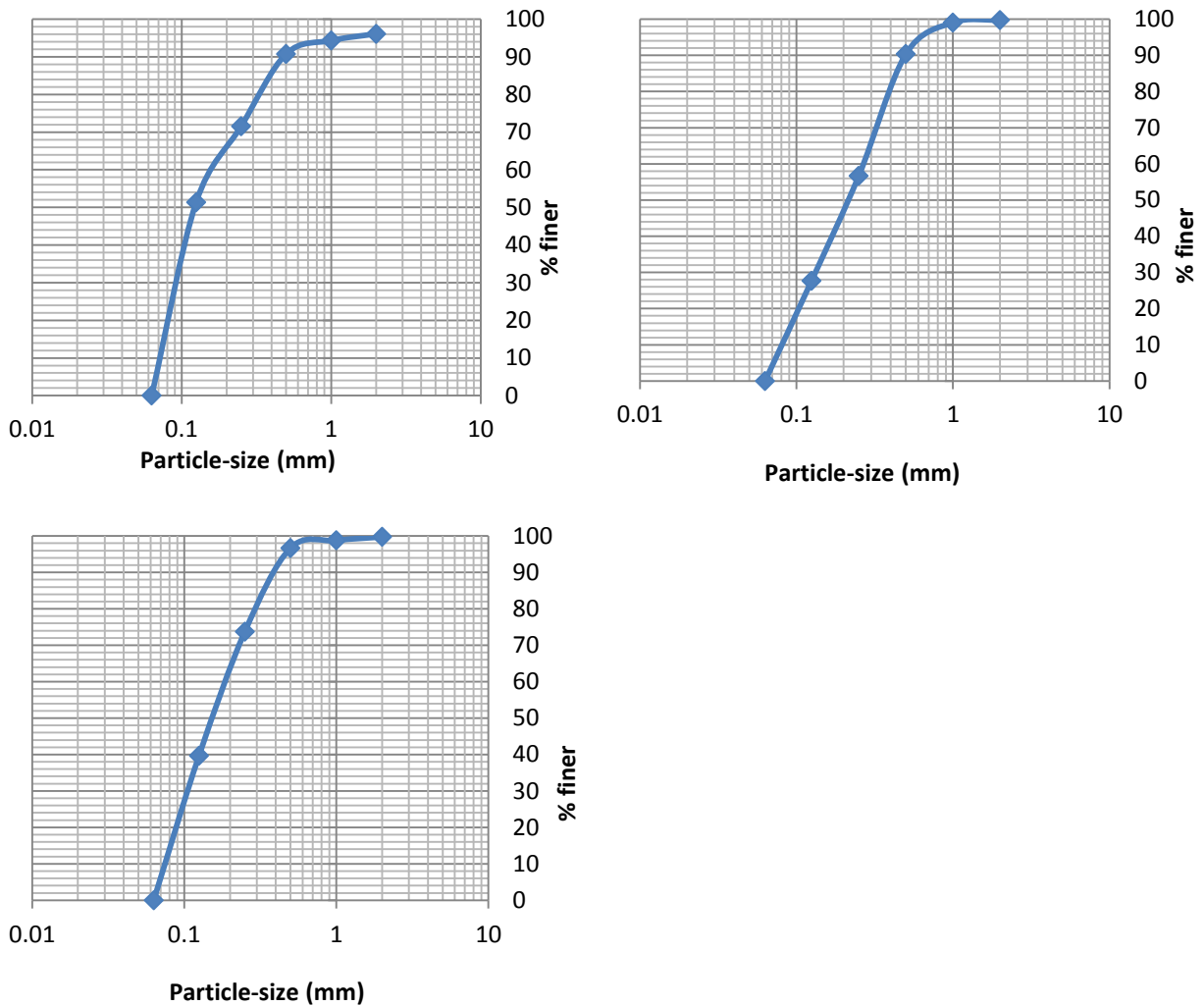


Figure 4.2 Percentage cumulative logarithmic curve showing grain-size distribution Mufulira outlet (Top left) and Uchi midpoint (Top right) and Uchi outlet (bottom right)

#### 4.1.3. Total metal distribution in different particle-size fractions

The results of the total metal concentrations of Co, Cu, Pb, Fe and Mn in the respective sediment fractions are presented in Fig 4.3a, Fig 4.3b and Fig 4.3c. Appendix C, Table C: 1 shows the analytical data for the total metal concentrations of the studied elements in the respective sediment fractions. Comparatively, the total metal concentrations in the whole sediment fraction were found to be higher than the amount detected in the coarser fractions but lower than finer fractions (Appendix C, Table C: 1). In the case of Co, highest values were found in UM2 and UO2 with corresponding concentrations as  $1000 \text{ mg kg}^{-1}$  and  $1500 \text{ mg kg}^{-1}$ . The remaining sampling locations recorded Co concentrations ranged from  $100 - 300 \text{ mg kg}^{-1}$  (Fig 4.3a). The total concentrations of Cu at all sampling sites ranged from  $500 \text{ mg kg}^{-1}$  at (KI3) to  $11200 \text{ mg kg}^{-1}$  at UM2. Sampling location KO1 recorded the highest concentrations for both Pb and Fe relative to all other sampling sites (Fig 4.3a). Mn concentrations were highest at MM4 and lowest at UM2.

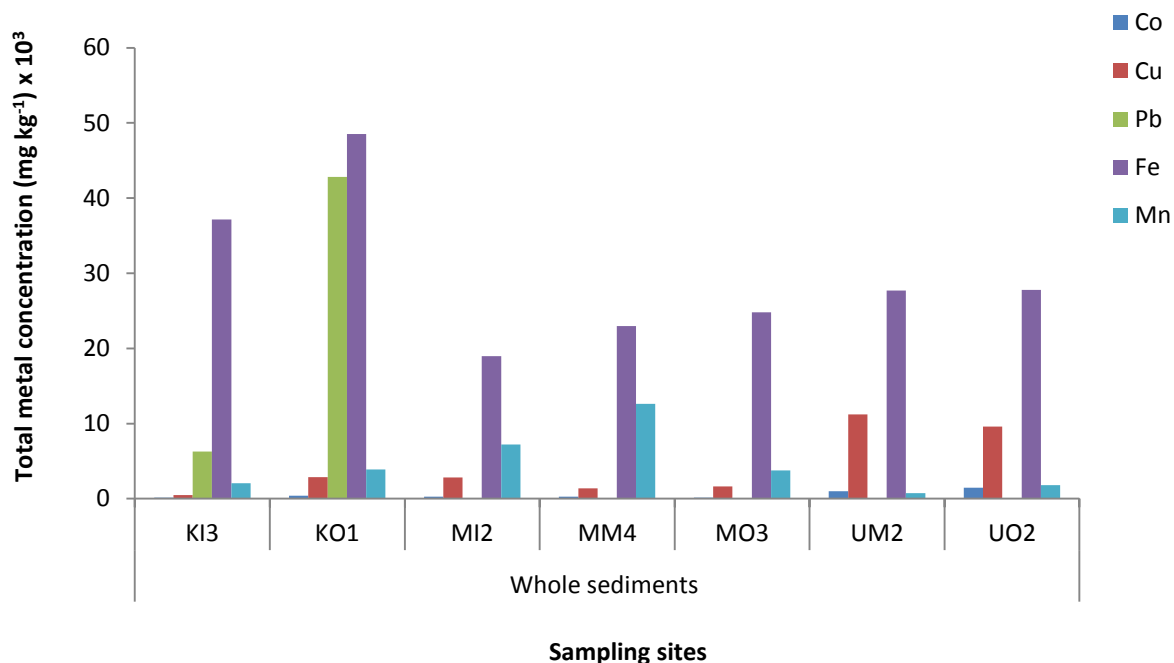


Figure 4.3a Results of total metal concentration ( $\text{mg kg}^{-1}$ ) in the whole sediment fraction

From Fig 4.3b, the total metal concentration of Co in the wetland sediment fraction  $< 63 \mu\text{m}$  is characterised by the highest levels at sampling stations UM2 and UO2 with concentrations of  $2400 \text{ mg kg}^{-1}$  and  $2100 \text{ mg kg}^{-1}$  respectively. Copper recorded the highest concentration at UM2 followed by UO2 (Fig 4.3b). Kabwe inlet (KO1) recorded the highest total concentrations of Pb in comparison to other sampling stations. Figure 4.3b also shows that Fe has high concentration at all sampling points although its concentration is more pronounced at KO1. Location MM4 recorded the highest concentration of Mn with UM2 recording the least.

Sediment fraction  $> 63 \mu\text{m}$  size recorded similar metallic characteristics as in particle size  $< 63 \mu\text{m}$  in all the sampling sites (Fig 4.3c). However, metallic concentrations are extremely higher in finer than in coarser fractions with the exception Fe at KI3, and Pb and Fe at KO1. The metal concentrations of Cu in coarser sediment fractions were found to vary across a broad range. Copper concentrations at UM2 ( $5500 \text{ mg kg}^{-1}$ ) and UO2 ( $4200 \text{ mg kg}^{-1}$ ) were found to be higher than other sampling points although the remaining locations with the exception of KI3 also recorded appreciation Cu concentrations (Fig 4.3c). Concentrations of Co were the lowest compared to that of the other measured elements (Fig 4.3c). Location UO2 recorded the highest Co concentration while the least concentration was found at KI3.

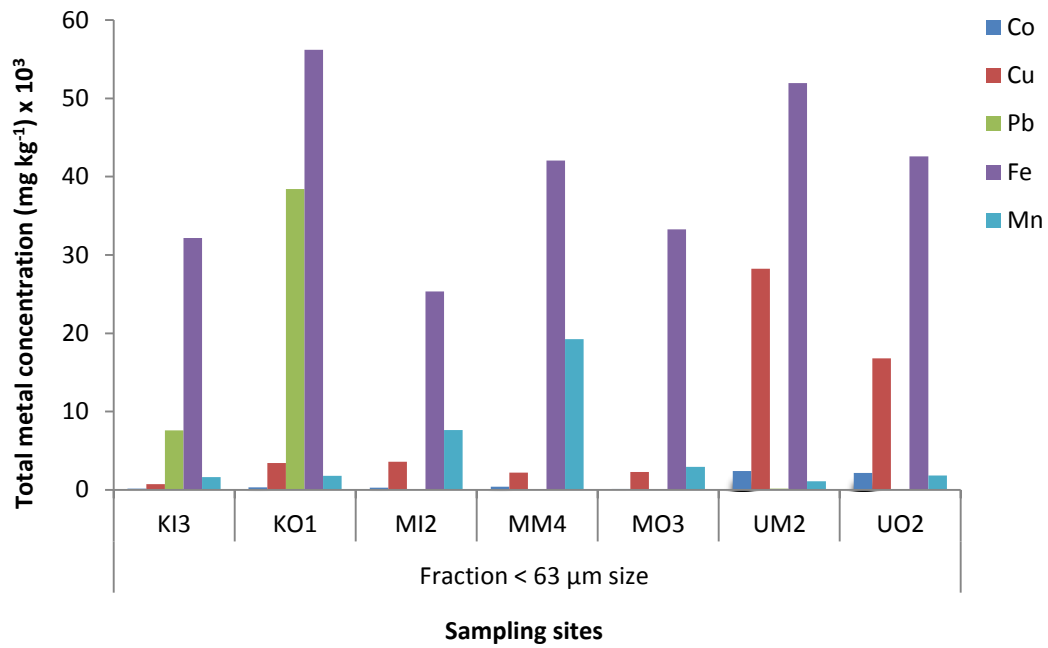


Figure 4.3b Results of total metal concentration (mg kg<sup>-1</sup>) in sediment fraction < 63 μm size

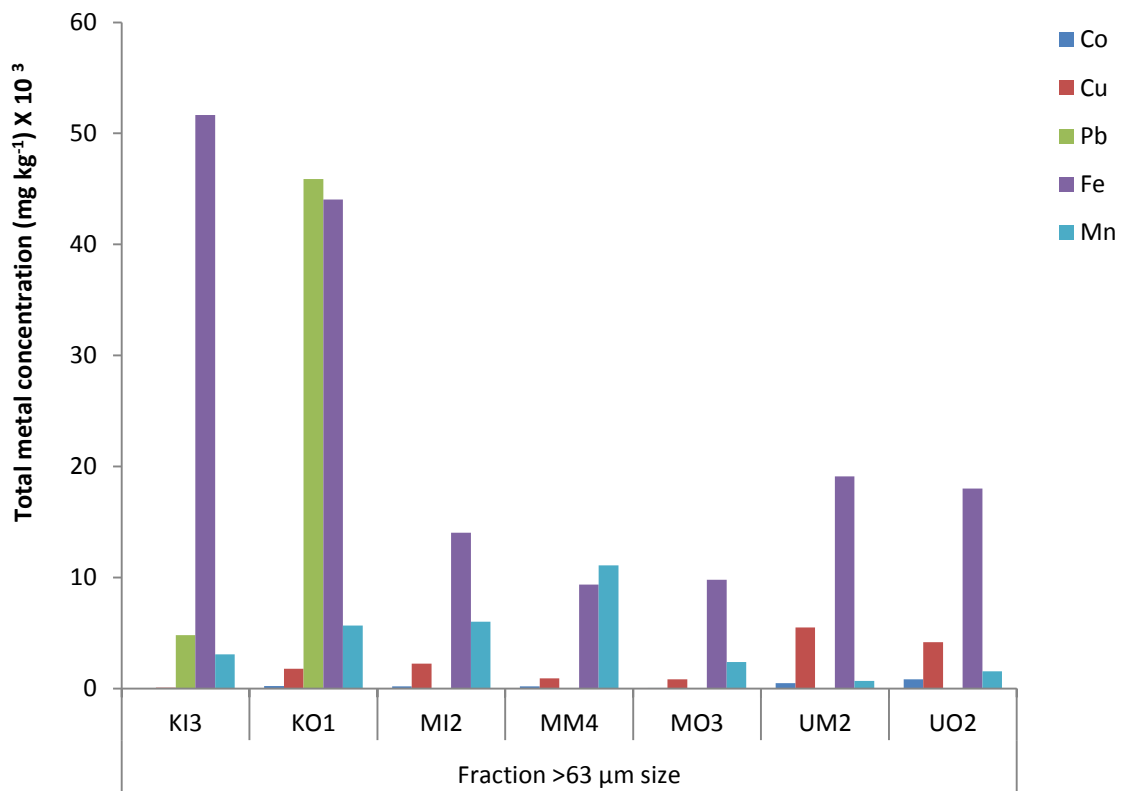


Figure 4.3c Results of total metal concentration (mg kg<sup>-1</sup>) in sediment fraction > 63 μm size

Table 4.3 Results for percentage recovery rates in the respective sediment particle-size fractions (Laboratory replicates, n = 3)

Site	Whole sediment (% Recovery)					Fraction < 63 µm (% Recovery)					Fraction > 63 µm (% Recovery)				
	Co	Cu	Pb	Fe	Mn	Co	Cu	Pb	Fe	Mn	Co	Cu	Pb	Fe	Mn
KI3	152	134	140	120	127	112	118	103	109	112	128	119	98	107	102
KO1	161	133	100	133	149	110	114	91	121	111	130	122	113	130	114
MI2	143	148	173	134	155	105	113	105	124	107	121	107	154	123	83
MO3	138	141	127	126	97	107	112	105	116	113	123	109	119	106	90
MM4	133	130	127	121	126	134	129	117	124	129	121	102	117	104	111
UM2	120	123	117	133	126	125	131	130	125	132	118	107	102	130	105
UO2	122	123	115	119	122	124	129	119	122	131	123	114	108	114	100

Table 4.3 shows the percentage recovery rates of the selected metals in the three sediment fractions. The recoveries for the whole sediment, < 63 µm and > 63 µm fractions ranged from 97-149 %, 91-132 % and 83-130 % respectively.

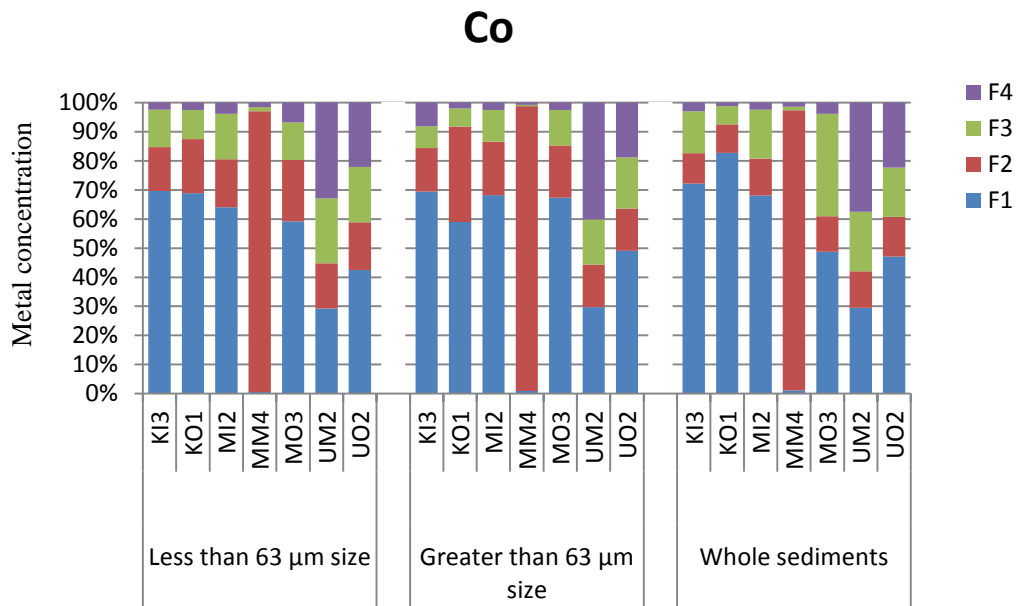
#### 4.1.4. Mass balance analysis

Using the total metal concentrations, the mass balance for the particle-size fractions was evaluated. This was done to assess if metal concentrations in both finer and coarser fractions equals that in the whole sediments (Appendix D; Table D: 1). Results indicate that the percentage mass balance ranged from 71 - 109 % for Co, 90 - 106 % for Cu, 95 - 181 % for Pb, 96 - 109 % Fe and 78 - 113 % for Mn. In general, the observed percentage mass balance indicates good metal recovery rates in both finer and coarser fractions in comparison to the metal concentrations in the whole sediment fractions.

#### 4.1.5. Metal fractions in different particle-size fractions of the studied sediments

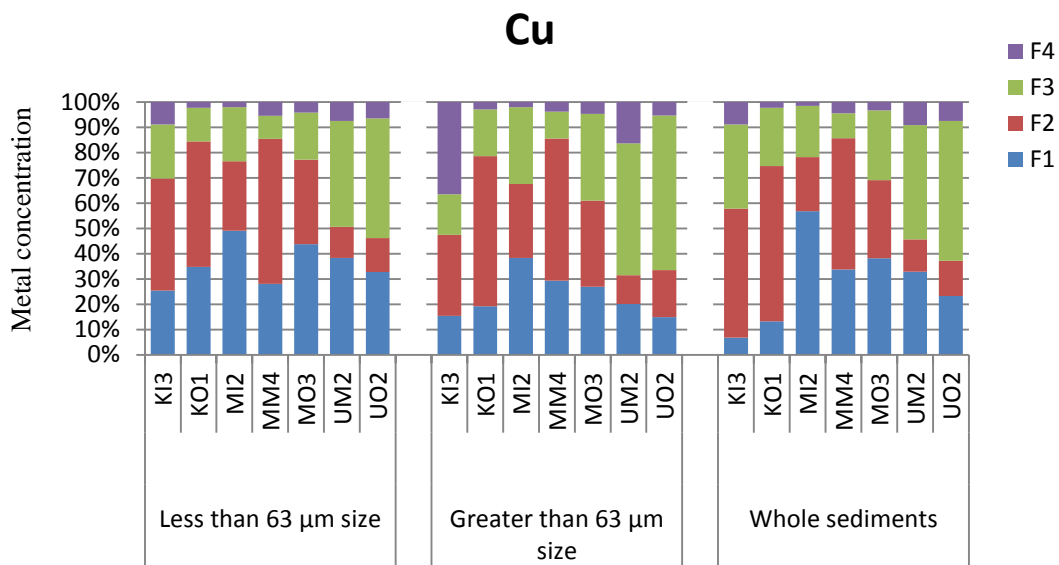
The results of metal fractionation in the different sediment particle-size distribution following the BCR sequential extraction procedures are shown in Fig 4.4a to Fig 4.4e. Appendix E shows the percentage distributions of the selected metals in their respective binding sites and the different sediment particle-size fractions. Metals are partitioned differently according to their preferred binding sites.

With the exception of location MM4, the acid-soluble fraction (F1) of Co dominated all other fractions in almost all particle-size distributions in all locations (Fig 4.4a). The lowest concentration (29 %) was recorded in particle-size < 63 µm at (UM2) and the highest (83 %) in the whole sediment at KO1 (Fig 4.4a). The reducible phase (F2) of Co at MM4 was the highest in all the three different particle-size fractions. The concentrations were, 97 %, 98 % and 96 % for < 63 µm, > 63 µm and the whole sediment particle-size fractions respectively. The oxidizable fraction of Co recorded the highest concentration (35 %) in the whole sediment at MO3 (Fig 4.3a). For the inert fraction of Co, the highest and the least concentrations of 40 % and 0.7 % were recorded in sediment fraction > 63 µm size at locations UM2 and MM4 respectively.



Sampling sites and grain-size distribution

Figure 4.4a Results of BCR sequential extraction partitioning ( $\text{mg kg}^{-1}$ ) and distribution of Co in the sediment samples



Sampling sites and grain-size distribution

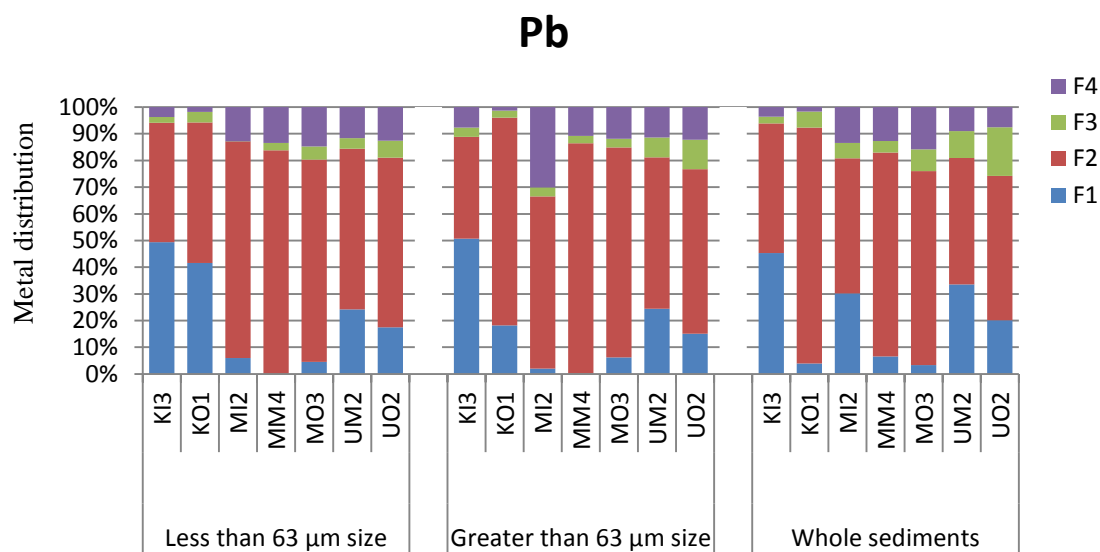
Figure 4.4b Results of BCR sequential extraction partitioning ( $\text{mg kg}^{-1}$ ) and distribution of Cu in the sediment samples

The fractions of Cu bound to Fe and Mn oxides (F2) were relatively the dominant phase in the respective particle-size fractions at all locations (Fig 4.4b). In particle size  $< 63 \mu\text{m}$ , the reducible fraction of Cu recorded the highest concentration (57 %) at MM4 with the least (12 %) at UM2. The exchangeable and the carbonate bound fractions (F1) of Cu recorded the highest concentration (49 %) at MI2 while 25 % of Cu was the least recorded at KI3. The amount of Cu bound to organic matter and sulphides (F3) recorded the highest concentration (47 %) in particle size  $< 63 \mu\text{m}$  at UO2. However, location MM4 recorded the least

(9 %) amount of oxidizable fraction of Cu in the same particle size fraction. The residual fraction (F4) of Cu recorded the highest concentration (9 %) at KI3 while the least (2 %) was recorded at MI2 and KO1 in the sediment particle size fraction < 63 µm.

The exchangeable and the carbonate fractions of Cu in sediment fraction > 63 µm recorded the highest concentration (38 %) at MI2 with the least concentration (15 %) at UO2 (Fig 4.3b). The reducible fraction of Cu had the highest concentration (59 %) at KO1 with the lowest concentration (11 %) at location UM2. Copper fraction bound to organic matter and sulphides recorded the highest concentrations (52 %) at UM2 while location MM4 recorded the least (10.67 %) of oxidizable fraction of Cu. Residual fraction in particle size > 63 µm recorded the least concentration compared to the preceding fractions. The highest inert concentration of Cu (36 %) was recorded at KI3 with the lowest (2 %) at location MI2.

Generally, fractions of Cu following the BCR sequential extraction in the whole sediment fraction did not differ from the above two (< 63 µm and > 63 µm size) fractions (Fig 4.3b). The highest acid-soluble fraction (57 %) of Cu was recorded at location MI2 with the lowest (7 %) at KI3. The highest and the least concentrations 61 % and 13 % of reducible fraction of Cu were recorded at KO1 and UM2 respectively while the oxidizable fraction had the highest concentration (55 %) at UO2 and the lowest (10 %) at location MM4. The residual fraction of Cu recorded the highest concentration (9 %) at location UM2 and the least concentration (2 %) at MI2 (Fig 4.4b).

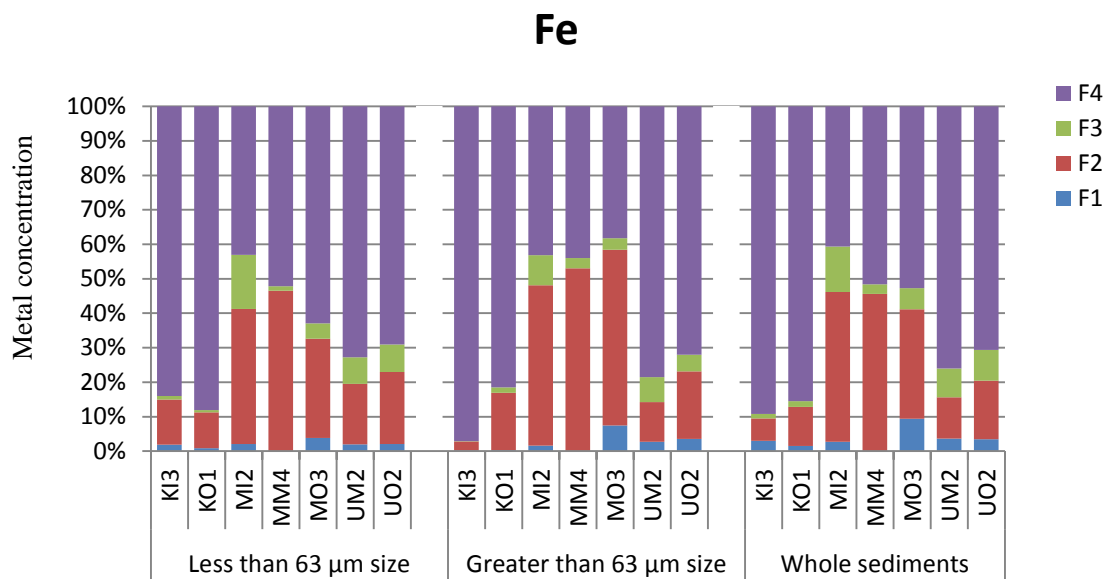


Sampling sites and grain-size distribution

Figure 4.4c Results of BCR sequential extraction partitioning (mg kg<sup>-1</sup>) and distribution of Pb in the sediment samples

Figure 4.4c gives the relative distribution of Pb in the different sediment particle-size fractions. The highest acid-soluble phase (F1) of Pb in all the three different particle-size fractions was recorded at location KI3. Interestingly, there was consistent decline in amount of Pb extracted from the acid-soluble phase to the oxidizable phase at KI3 in sediment fractions, < 63 µm and > 63 µm sizes (Appendix E, Table E: 3). Location MM4 recorded the least (0.03 %) acid-soluble phase of Pb in fraction < 63 µm compared to all sediment fractions. Meanwhile, in both particle-size fractions < 63 and > 63 µm, the highest amounts of the

reducible phase of Pb were recorded at location MM4 with concentrations as 84 % and 86 % respectively. Generally, location KO1 of whole sediment fraction recorded the highest (88 %) reducible phase of Pb in all sediment fractions in comparison to all other locations (Appendix C, Table E: 3). Fractions of Pb bound to organic matter and sulphides (F3) were relatively the lowest phase of all the four fractions. The highest amount of oxidizable fraction (18 %) of Pb was recorded at UO2 of whole sediment fraction while in sediment fraction < 63  $\mu\text{m}$ , location MI2 recorded the least (0.02 %). The highest residual fraction of Pb was recorded at location MI2 of particle size > 63  $\mu\text{m}$  while the least amount was recorded at KO1 of the same particle size fraction (Fig. 4.4c and Appendix E, Table E: 3).



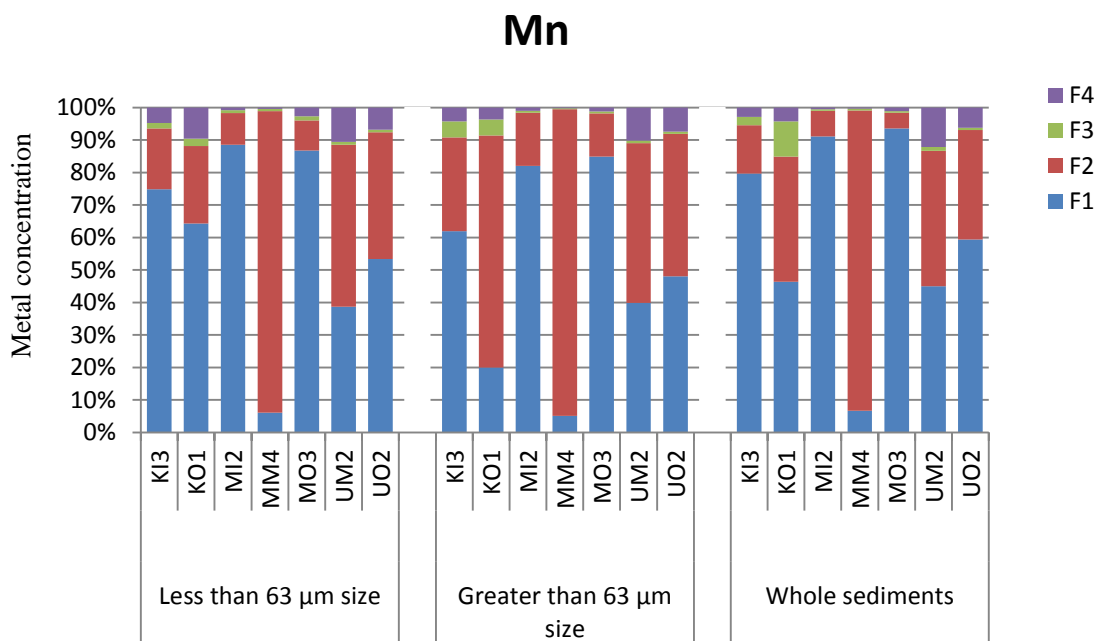
Sampling sites and grain-size distribution

Figure 4.4d Results of BCR sequential extraction partitioning ( $\text{mg kg}^{-1}$ ) and distribution of Fe in the sediment samples

From Fig 4.4d, it can be observed that Fe is much concentrated in the residual phase in all sediment particle size fractions and at all locations. In comparison to other sediment fractions, the highest inert fraction (97 %) of Fe was recorded at KI3 and the lowest (38 %) at MO3 in sediment fraction > 63  $\mu\text{m}$  size (Fig 4.4d and Appendix E, Table E: 4). The highest and the lowest concentration of residual phase of Fe in sediment particle size fraction < 63  $\mu\text{m}$  were (88 %) and (43 %) recorded at KO1 and MI2 respectively. The whole sediment recorded the highest (89 %) residual fraction of Fe at location KI3 and the lowest (41 %) concentration at MI2. Location MI2 recorded the highest oxidizable phase of Fe in all the three sediment fractions. The respective percentage concentrations were 9 %, 13 % and 16 % for particle size fraction > 63  $\mu\text{m}$ , whole sediment and fraction < 63  $\mu\text{m}$  size (Fig 4.4d and Appendix E, Table E: 4).

The highest reducible phase of Fe was recorded at MM4 of all the three sediment particle-size fractions compared to all other sampling stations (Fig 4.4d and Appendix E, Table E: 4) Meanwhile, location KI3 recorded the lowest reducible phase of Fe in both particle-size fractions > 63  $\mu\text{m}$  and the whole sediment fractions with concentrations 3 % and 7 % respectively. Location KO1 recorded the lowest (10 %) reducible phase of Fe in particle-size fraction < 63  $\mu\text{m}$  size.

Comparatively, the acid-soluble fraction of Fe was the lowest fraction of all the four phases of Fe in all particle-size fractions at all locations (Fig 4.4d). Location MM4 recorded the lowest acid-soluble phase of Fe in all the three particle size fractions. The acid-soluble phases (F1) of Fe recorded at location MM4 for all the three different sediment particle-size fractions were as follows 0.0 %, 0.1 % and 0.1 % for sediment fraction < 63  $\mu\text{m}$ , whole sediment and the fraction > 63  $\mu\text{m}$  size respectively. Compared to all locations, MO3 recorded the highest acid-soluble phase of Fe in all the three sediment particle-size fractions with corresponding concentrations as 4 %, 8 % and 9 % for fraction > 63  $\mu\text{m}$ , < 63  $\mu\text{m}$  and the whole sediment fractions. The highest oxidizable phase of Fe was observed at sampling site MI2 in all the three particle-size fractions (Appendix E; Table E: 4). From the data set, it is possible to establish the following order for the different phases of Fe in the three different sediment fractions as follows: residual > reducible > oxidizable > acid soluble. The phases of Fe followed similar distribution pattern in all the three sediment fractions. However, individual sampling points exhibited slightly different distribution pattern.



Sampling sites and grain-size distribution

Figure 4.4e Results of BCR sequential extraction partitioning ( $\text{mg kg}^{-1}$ ) and distribution of Mn in the sediment samples

Fractions of Mn following BCR sequential extraction are presented in Fig 4.3e. Location MO3 recorded the highest acid-soluble phase of Mn in sediment particle size fraction > 63  $\mu\text{m}$  while MI2 had the highest (89 %) acid-soluble phase in fraction < 63  $\mu\text{m}$  size. Meanwhile, location MM4 recorded the lowest exchangeable and the carbonate bound fractions of Mn in sediment fraction < 63  $\mu\text{m}$  and > 63  $\mu\text{m}$  sizes with corresponding concentrations as 6 % and 5 %. The acid-soluble phase of Mn in the whole sediment fraction ranged from 7 % to 80 % (Fig 4.4e).

The reducible fraction of Mn ranged from 5 % at (MO3) to 92 % at (MM4) in the whole sediment (Fig 4.4e and Appendix E, Table E: 5). The sediment fraction > 63  $\mu\text{m}$  size recorded the highest (94%) reducible fraction of Mn at MM4 and the lowest (13 %) at MO3. Similar observation was made in Particle-size fraction < 63  $\mu\text{m}$  (Appendix E, Table E: 5).

The highest oxidizable phase of Mn of all the sediment particle size fractions was recorded at KO1 (11 %) in the whole sediment fraction. However, two locations, MI2 and MO3 recorded the same concentrations of oxidizable phase of Mn in the whole sediment fraction. Their concentration (0.5 %) was the third lowest after 0.3 % at MM4 in particle size >63 µm fractions compare to all other locations. The sediment fraction > 63 µm recorded the highest (5 %) oxidizable fraction of Mn at KI3 and KO1 while locations MI2 and MO3 recorded the lowest (0.6 %). Similar trend was observed in the sediment particle size fraction < 63 µm size (Appendix C, Table C: 5). The residual fraction of Mn recorded the highest concentrations in all the three sediment fractions at UM2. At location UM2, sediment fraction < 63 µm recorded 11 %, while fraction > 63 µm and the whole sediments recorded 10 % and 12 %, respectively.

#### 4.1.6. Assessment of potential toxicity of heavy metals in sediment

Appendix F; Table F: 1 gives the percentage acid-soluble fraction in total metal concentration for potential risk assessment of metals in the studied sediments. The risk assessment code which mainly applies to the exchangeable and the carbonate bound fractions was used to evaluate potential metal toxicity in the wetland environments. With the exception of sampling location MM4, Mn was found to be of extreme risk to the environment in all other stations in the whole sediment fraction (Fig 4.5a). The mobility of Mn in the respective sampling sites follows the order KI3 (95 %)> MO3 (87 %)>MI2 (81 %)>UO2 (72 %)>KO1 (69 %)> UM2 (57 %)> MM4 (8 %) (Fig. 4.5a). At sampling site MM4 (8 %), Mn was found to be of low risk to the environment. Cobalt was found to be very high risk to the environment at stations KO1, MI2, KI3, MO3 and UO2, of high risk at UM2 and of low risk at MM4 (Fig 4.5a). Copper showed varied levels of risk to the environment. At sampling stations MI2 and MO3, Cu was found to be of extreme risk for the environment with percentage risk assessment code of 84 % and 54 % respectively. Stations UM2 and MM4 recorded high risk levels of Cu while KO1 and UO2 recorded medium risks. Sampling location KI3 (9 %) was found to have low mobility of Cu. Pb was found to be very high risk at stations KI3 and MI2, of high risk at station UM2, of medium risk at UO2 and of low risk at stations MO3, KO1 and MM4 (Fig. 4.5a). The Fe was non-risky at location MM4 (0.10 %), of medium risk at location MO3 (12 %) and of low risk at locations KI3 (4 %), KO1 (2 %), UM2 (5 %), UO2 (4 %) and MI2 (4 %).

From Fig 4.5b it can be seen that the percentage concentration of the acid-soluble fractions (F1) in the total metal concentrations of Mn, Co, Cu, Pb and Fe, were 8 - 99 %, 0.8 - 78 %, 30 - 55 %, 0.03 - 51 % and 0.05 - 4 % respectively. This suggests that, Mn may posed very high risk to the environment followed by Co. Copper was found risky to the environment with a high risk level at all other stations except KI3 (medium toxicity). Pb only posed very high risk to the environment at KI3, while locations KO1 and UM2 recorded high Pb risk levels, MI2 and MO3 low risk, and UO2 medium risk.

Similar but a reversed risk assessment of studied metals to the environment was observed in sediment particle-size fraction > 63 µm (Fig 4.5c). Cobalt was found to be of extreme risk for the environment at stations KI3, MI2, MO3, KO1 and UO2 (89 - 60 %), of high risk at sampling site UM (35 %) and of low risk at location MM4 (1 %). Mn was found to be extremely risky to the environment at KI3, MI2 and MO3 (63 - 77 %), of high risk at location UM2 and UO2 (42 - 48 %), of medium risk at KO1 (23 %) and of low risk at location MM4 (6 %). Copper was only found to be high risk at MI2 with medium risk at the other locations. Pb exhibited variations between the sampling sites and was found to be high risk at KI3, of medium risk at KO1, UM2 and UO2 (16 - 50 %) and of low risk at MI2 and MO3 (3 - 7 %). At MM4, Pb was found to be of no risk to the environment (0.32 %). Fe was non-risky to the environment at KI3, KO1 and MM4 (0.06 - 0.09 %) and of low risk at the other sampling sites.

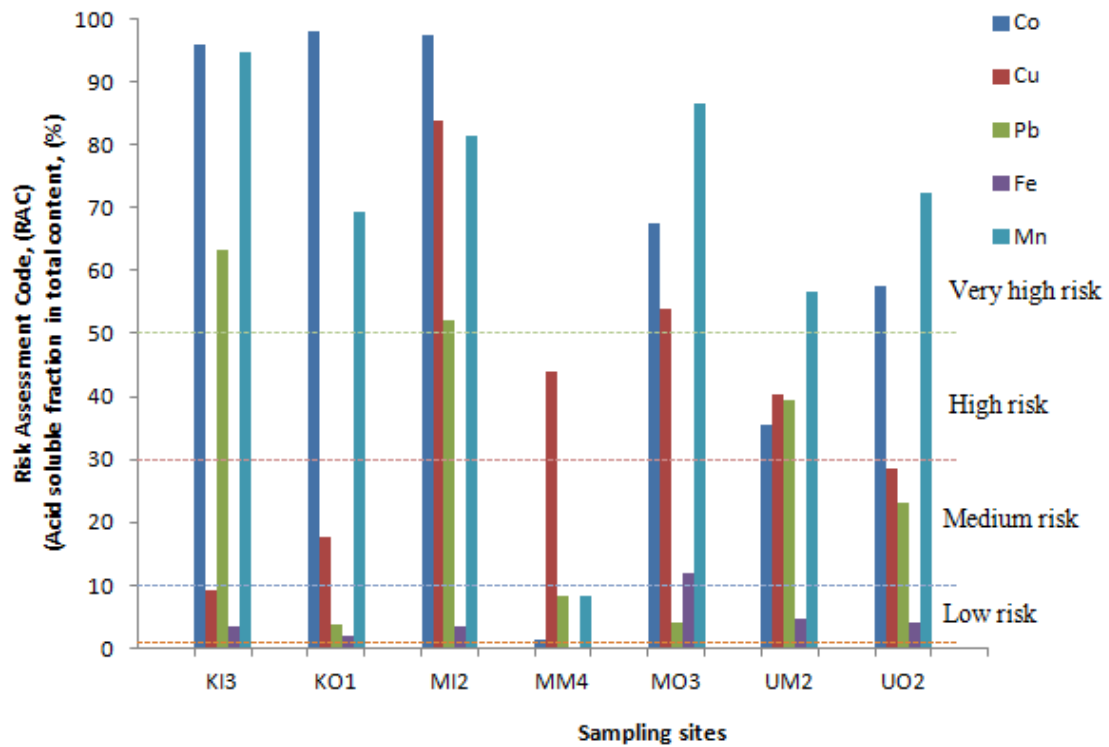


Figure 4.5a Risk Assessment Code for selected metals in whole sediment fraction

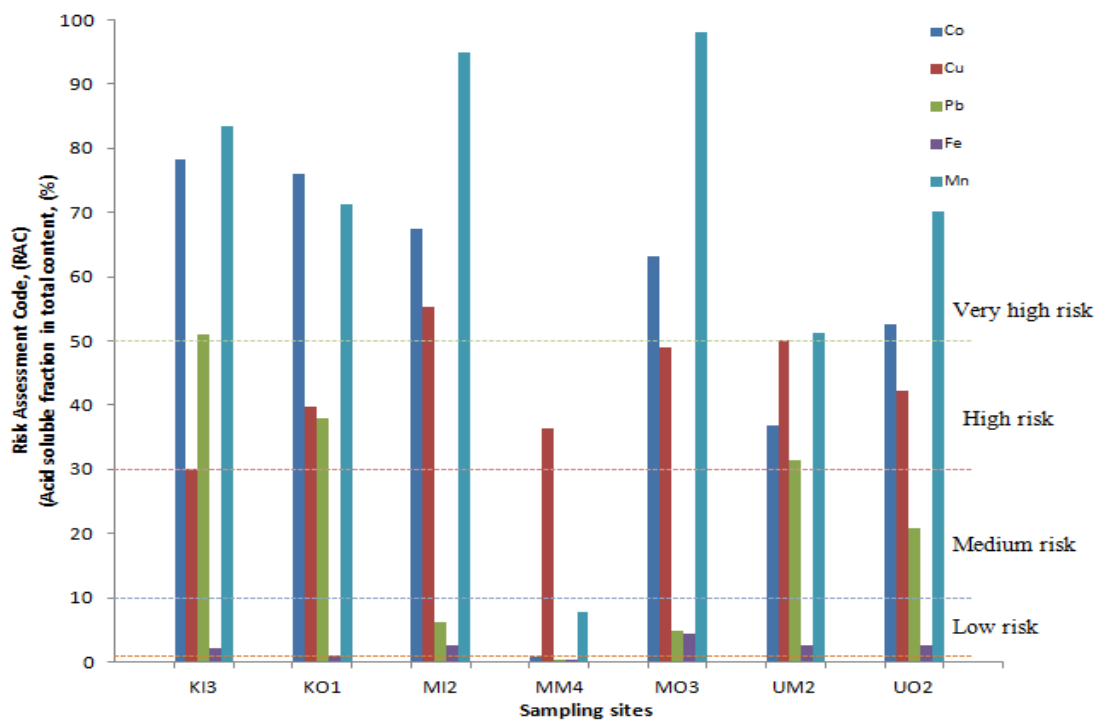


Figure 4.5b Risk Assessment Code for selected metals in sediment particle size fraction <math>< 63 \mu\text{m}</math>

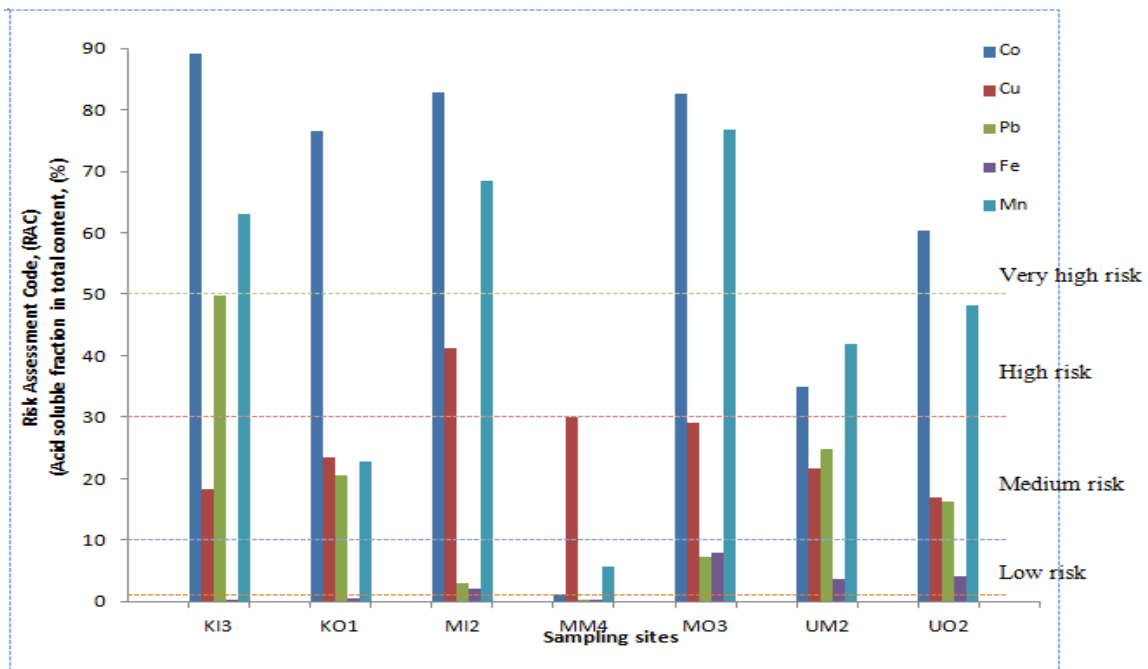


Figure 4.5c Risk Assessment Code for selected metals in sediment particle size fraction > 63 μm

#### 4.1.7. Assessment of sediment toxicity using Canadian Sediment Quality Guidelines (SQG)

Table 4.4 presents the total metal concentrations of Co, Cu and Pb together with the Threshold Effect Level (TEL) and the Probable Effect Level (PEL) values of the Canadian Sediment Quality Guidelines (Santos et al., 2013; Olofade et al., 2008). The adverse effect of Co to aquatic living resources could not be evaluated using the Canadian (SQG) because this SQG does not have threshold effect and probable effect levels for Co. Cu concentrations were generally above the PEL in the all three particle-size fractions at all sampling locations investigated. Potential adverse effects of Pb were mostly recorded at locations KI3 and KO1 in the three respective sediment fractions as Pb concentrations exceeded the PEL. The remaining locations recorded either uncertain or unlikely toxicity effects of Pb (Table 4.4).

Table 4.4 Total metal concentrations (mg kg<sup>-1</sup>) and Canadian sediment quality guidelines values (Laboratory replicates, n = 3)

	Site	Co	Cu	Pb
Fraction < 63 µm	KI3	170	710 <sup>c</sup>	7600 <sup>c</sup>
	KO1	320	3400 <sup>c</sup>	38000 <sup>c</sup>
	MI2	280	3600 <sup>c</sup>	40 <sup>d</sup>
	MO3	130	2300 <sup>c</sup>	50 <sup>d</sup>
	MM4	400	2200 <sup>c</sup>	60 <sup>d</sup>
	UM2	24000	28000 <sup>c</sup>	140 <sup>c</sup>
	UO2	2100	17000 <sup>c</sup>	90 <sup>d</sup>
Fraction > 63µm size	KI3	40	100 <sup>d</sup>	4800 <sup>c</sup>
	KO1	240	1800 <sup>c</sup>	46000 <sup>c</sup>
	MI2	210	2200 <sup>e</sup>	10 <sup>e</sup>
	MO3	60	830 <sup>c</sup>	20 <sup>e</sup>
	MM4	220	930 <sup>c</sup>	10 <sup>e</sup>
	UM2	500	5500 <sup>c</sup>	30 <sup>e</sup>
	UO2	850	4200 <sup>c</sup>	20 <sup>e</sup>
Whole sediment fraction	KI3	160	500 <sup>c</sup>	6300 <sup>c</sup>
	KO1	400	2900 <sup>c</sup>	43000 <sup>c</sup>
	MI2	250	2800 <sup>c</sup>	10 <sup>e</sup>
	MO3	130	1600 <sup>c</sup>	30 <sup>e</sup>
	MM4	260	1400 <sup>c</sup>	30 <sup>e</sup>
	UM2	1000	11000 <sup>c</sup>	60 <sup>d</sup>
	UO2	1500	9600 <sup>c</sup>	50 <sup>d</sup>
TEL <sup>a</sup>		-	35.7	35
PEL <sup>b</sup>		-	197	91.3

<sup>a</sup>TEL: Threshold effect level; <sup>b</sup>PEL: probable effect level; <sup>c</sup> possible toxicity; <sup>d</sup> uncertain toxicity effect; <sup>e</sup> unlikely toxicity effect

#### 4.1.8. Pearson correlation coefficient matrix for BCR extracted heavy metal concentrations and sediment physico-chemical characteristics

Pearson correlations between the mean values of sediment characteristics, metal fractions and total metal concentrations were investigated to determine the relationship between sediment physico-chemical characteristics and metal concentrations (Table 4.5). Table 4.5 shows the relationships between sediment properties and metals in all the three sediment particle-size fractions. While no linear relationship existed between moisture, temperature and fractions of Cu, Pb and Mn, a significant relationship was observed only between temperature and the F2 fraction of Co in all the sediment particle-size fractions (Table 4.5). Moisture also correlated positively with F2 and mobile fractions of Fe in both the whole sediment and the

sediment fraction > 63  $\mu\text{m}$  size while no correlation was observed between fractions of Fe and moisture in the particle-size < 63  $\mu\text{m}$ . Only F1 fraction of Mn in the sediment fraction > 63  $\mu\text{m}$  size showed positive significant correlation ( $r = .87^*$ ) with organic matter. Fractions of the remaining metals did not correlate significantly with organic matter.

Significant negative relationships existed between sediment pH and all fractions of Pb except F1 and F4 fractions in the whole sediment (Table 4.5). With the exception of F1 and F4 fractions, the F2 (reducible) ( $r = -.76^*$ ), F3 (oxidizable) ( $r = -.76^*$ ), mobile ( $r = -.76^*$ ) and the total concentration ( $r = -.76^*$ ) of Pb showed negative significant correlation with sediment pH in the coarser sediment fraction (Table 4.5). Only F3 fraction of Mn correlated negatively with pH in the whole sediment fraction while no correlation was observed between pH and fractions of Fe in all particle-size fractions. These negative relationships suggest possible increase mobility of Pb and the F3 fraction of Mn with decrease pH. The lack of significant correlation between pH and the acid-soluble phase of all the metals implies that this mobile phase of the metals is unlikely to pose environmental problem should there be a shift in sediment pH.

Organic matter, pH and EC revealed no significant relationship with fractions of Co, Cu and Fe. This indicates that, organic matter does not provide binding sites for Co, Cu and Fe. However, EC revealed positive linear relationship with most fractions of Pb in all the sediment particle-size fractions. F1 ( $r = 0.84^*$ ), F2 ( $r = 0.86^*$ ), F3 ( $r = 0.88^{**}$ ), F4 ( $r = .86^*$ ), Mobile ( $r = 0.86^*$ ) and total concentration ( $r = 0.86^*$ ) of Pb and the EC correlated positively in the finer fraction. In the sediment fraction > 63  $\mu\text{m}$  size, strong positive correlations existed between EC and all the fractions of Pb (Table 4.5). EC also revealed positive linear relationship with F2 ( $r = .88^{**}$ ), F4 ( $r = .78^*$ ), mobile ( $r = .86^*$ ), and the total concentration ( $r = .87^*$ ) of Pb in the whole sediment fraction. The oxidizable fraction of Mn correlated positively with EC in both the whole sediment and the sediment fraction > 63  $\mu\text{m}$  size but no linear relationship was observed between fractions of Mn and EC in the finer fractions (Table 4.5). These strong positive correlations between the mobile fractions of Pb, Mn and EC indicate that EC may be the main regulatory factor for Pb mobility in the sediments.

With the exception of oxidizable (F3) and the residual fractions (F4) of Co, CEC did not correlate with all other fractions of Co in the whole sediment fraction. Meanwhile, correlation between CEC and F1 ( $r = -.85^*$ ), F3 ( $r = -.94^{**}$ ), F4 ( $r = -.94^{**}$ ), mobile fraction ( $r = -.87^*$ ) and the total concentration ( $r = -.90^{**}$ ) of Co showed a strong negative linear relationship in the finer fractions. F3 and F4 fractions of Co also correlated negatively with CEC in the sediment fraction > 63  $\mu\text{m}$  size while other fractions showed no significant correlations with CEC. Correlations between CEC and F1 ( $r = -.95^{**}$ ), F3 ( $r = -.91^{**}$ ), mobile fraction ( $r = -.93^{**}$ ), F4 ( $r = -.93^{**}$ ) and the total concentration ( $r = -.93^{**}$ ) of Cu were observed to be significant in the whole sediment fractions. Meanwhile, all fractions of Cu in the finer sediment fractions showed negative significant correlation with CEC. In the sediment particle-size fraction > 63  $\mu\text{m}$  size, all fractions with the exception of F2 of Cu showed negative significant correlations with CEC. However, CEC only showed a strong positive linear relationship with F3 fraction of Pb in the whole sediment fraction, while all other fractions revealed no significant correlation with CEC. Also CEC showed negative significant correlation with F3 fraction of Fe in both whole sediment fraction ( $r = -.81^*$ ) and the fraction < 63  $\mu\text{m}$  size ( $r = -.86^*$ ). F3 fraction of Mn revealed positive correlation with CEC in the fraction > 63  $\mu\text{m}$  size. The CEC as a regulator of metal mobility in sediments may therefore be the main factor controlling fractions of Co, Cu and the oxidizable phases of Fe and Mn in the sediments. The residual phases of both Co and Cu showing negative significant correlations with CEC indicate that increase CEC may be due to a release of these metals from the residual phase of the sediments.

Table 4.5 Pearson correlations for sediment physico-chemical characteristics and BCR extracted selected metal concentrations for whole sediment fraction, sediment fractions < 63 µm, and > 63µm (Laboratory duplicates, *n* = 2).

Metal	Sediment characteristics	Whole sediment fraction						Sediment fraction < 63 µm						Sediment fraction > 63 µm					
		Fractions				mob	Total	Fractions				Mobile	Total	Fractions				Mobil	Total
		F1	F2	F3	F4			F1	F2	F3	F4			F1	F2	F3	F4	e	
Co	Moisture (%)																		
	Temperature (°C)		.87*						.76*					.79*					.77*
	pH																		
	LOI (%)																		
	EC µS/cm																		
	CEC meq Na/100 g			-.90**	-.93**	.04	-.52	-.85*	-.49	-.94**	-.94**	-.87*	-.90**	-.57	.08	-.77*	-.93**	-.54	-.71
Cu	Moisture (%)																		
	Temperature (°C)																		
	pH																		
	LOI (%)																		
	EC µS/cm																		
	CEC meq Na/100 g		-.95**	-.91**	-.93**	-.93**	-.93**	-.94**	-.80*	-.94**	-.92**	-.93**	-.94**	-.81*		-.94**	-.86*	-.87*	-.91**
Pb	Moisture (%)																		
	Temperature (°C)																		
	pH		-.76*	-.76*		-.76*	-.76*							-.76*	-.76*			-.76*	-.76*
	LOI (%)																		
	EC µS/cm		.88**		.78*	.86*	.87*	.843*	.86*	.88**	.77*	.86*	.86*	.85*	.85*	.88**	-.54	.88**	.88**
	CEC meq Na/100 g			.88**															

Table 4.5 (Cont...)



#### 4.1.9. Similar characteristics in metallic concentrations in sampling stations

Employing Statistical Package for Social Sciences (SPSS) version 16, a hierarchical cluster analysis using Ward's method and euclidean distance approach was used to identify areas of similar characteristics of metallic concentrations (Fig. 4.6). Sampling sites were grouped according to similarity in total metal concentrations in the whole sediment fraction. Whole sediment fraction was selected because aquatic biota are exposed to the whole sediment and not just to particular grain-size fractions (Akhurst et al., 2011). The dendrogram showed three different groups for total metal concentrations for all sampling sites. Sampling sites in each group exhibit similar metallic properties and anthropogenic sources of the metals. Group I consists of only station KO1 and represent the highly polluted site with the highest Pb pollution (Fig. 4.3a). Group II stations (UM2 and UO2) were highly polluted with Cu (Fig. 4.3a). A major cluster (Group III) which includes stations MO3, MM4, MI2 and KI3 was observed. This cluster was the third heavy metal contaminated sites (Fig. 4.3a). The pollution in these sites aroused from seepage and erosion of metals from abandon tailings dams containing different kinds of metals (Table 3.1). All sampling sites (Group I, II and III) may be characterised by anthropogenic metal input.

#### 4.1.10. Similar characteristics in metallic concentrations in sampling stations

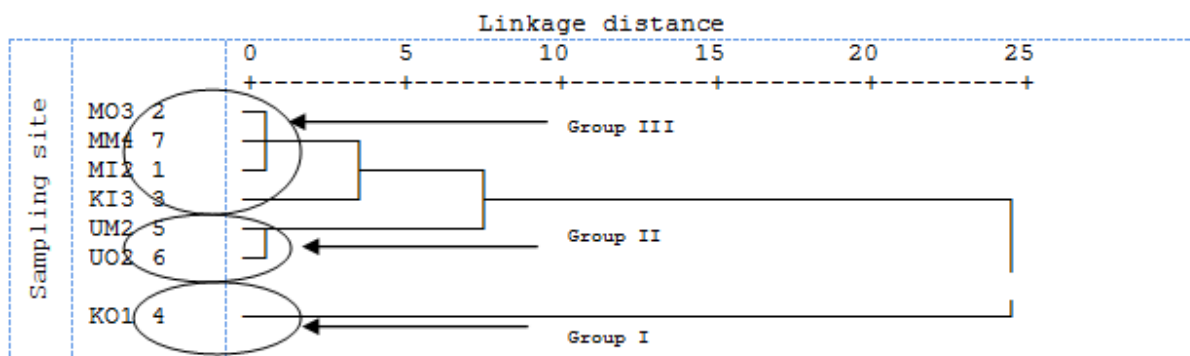


Figure 4.6 Dendrogram indicating similarity in metallic concentration among the sampling sites

## CHAPTER 5

# Discussion

---

### 5.1. Total metal concentrations, percentage recovery rates and mass balance

Total metal concentrations in the investigated sediment particle-size fractions at the various sampling sites varied in a broad range of values (Figs 4.4a, 4.4b and 4.4c). Results indicate that, in general, total metal concentrations in the respective particle-size fractions were higher in the finer fractions than both the whole sediments and the fractions > 63  $\mu\text{m}$  size. This observation confirms the assertion that, finer fractions adsorb greater proportion of metals at its mineral surfaces due to its large surface area (John & Leventhal, 1995; Horowitz, 1985) compared to coarser fractions. The results are in conformity with the findings of (Zhao et al., 2010). Studies by Sracek et al. (2012) on metal distribution in river sediments within the Copperbelt reported concentrations of Co within the ranges of 330 -1400  $\text{mg kg}^{-1}$  while Cu recorded concentrations from 100 - 3200  $\text{mg kg}^{-1}$ . Fe and Mn had concentrations within the ranges of 25000 - 56000 and 270 - 160  $\text{mg kg}^{-1}$ , respectively. In their studies concentrations of Pb were not investigated. Comparing the concentrations of the respective elements in the current study (Appendix C, Table C: 1 ) to studies by Sracek et al. (2012), it can be observed that heavy metal concentrations within the Copperbelt has greatly increased. These higher metal concentrations within the study area are indicative of anthropogenic sources for the selected elements into the environment. This result agrees with reports by Sracek et al. (2012). However, in comparison to the coarser fractions, the whole sediments recorded relatively higher metal concentrations. (Fig. 4.3a and Fig. 4.3c). On based on these findings, it can be suggested that, the whole sediment fraction exhibited an average behaviour in terms of its metal accumulation capacity in comparison to both the finer and the coarser sediment fractions.

The relatively high metal recovery rate observed in this study can be attributed to the possible contamination resulting from the various steps in the BCR procedure. Similar observations have been published by other researchers (Kartal & Birol, 2003; Fernandez et al., 2004). The higher recoveries can also be attributed to the heterogeneity of the sediments in terms of their high pollution loadings despite repeated attempts to homogenize the sediments by grinding into fine power (Kabala et al., 2011). This observation together with the relatively higher mass balance for Pb recorded at MI and MO3 (Appendix D) can be attributed to the high variability of Pb in sediments. Similar observation had been published by

Tessier et al. (1979) where high variabilities in Pb concentrations were attributed to relatively large (> 8 µm) lead-rich particles in sediments.

## 5.2. Metal distribution

### 5.2.1. Exchangeable fraction and fraction bound to carbonate (Acid-soluble, F1)

The acid-soluble phase of Co in the whole sediment fraction ranged from 1.1 - 82.8 % (Appendix E, Table E: 1). However, sediment finer fractions recorded Co concentrations in the acid-soluble phase within the ranges of 0.6 - 69.7 %. Comparatively, Co fractions bound to exchangeable and the carbonates were higher in the whole sediment than the finer. However, when Co concentration in the finer fractions are compared with concentrations reported in other studied, relatively high percent of exchangeable and carbonate bound fractions of Co was observed in this study (Tessier et al., 1979). Tessier et al. (1979) reported concentration of Co in the carbonate fraction below detection limit. This disparity may be due to differences in environmental conditions such geology, redox potential etc. in difference study areas and the state of sediments used for the analysis. However, the relatively high Co fraction bound the carbonate indicates that, Co has the potential to pose serious threat to the aquatic biota in these sampling sites. Compared to the sediment fraction < 63 µm size, particle size > 63 µm size has limited ability to adsorb metals. However, the acid soluble fraction of Co in the coarser fraction is comparable to the amount in the finer fraction for all the sampling sites (Appendix E, Table E: 1) (Fig 4.4a). Cobalt therefore seems to have strong affinity to be bound to the carbonate binding site of the studied sediments as opposed to Fe and Mn oxides. This finding is in contradiction to reported literature on binding sites for cobalt (Krupka & Serne, 2002; Howe et al., 2006). Fe/Mn oxides (Sracek et al., 2012) and the organic matter and sulphide fractions (Sungur et al., 2014) have been reported as the main binding sites for Co, which is contrary to the result in the current study.

Distribution of acid-soluble phase of Cu in the whole sediment fraction ranged from 7-57 % at all sampling sites (Appendix E, Table E: 2). The highest concentration was observed at sampling site MI2 (Fig 4.4b). Other sampling stations recorded concentrations within the ranges of 7 % and 38 %. In general, sediment particle-size < 63 µm size, recorded higher fractions of carbonate bound Cu (25 % - 49 %) in this study compared to the amount (10 - 25 %) reported by (Wang et al., 2010). Generally, lowers (13 % - 16 %) fractions of Cu associated with carbonates have also been reported by Tessier et al 1979. This revealed that the mineral composition of the sediments for this current study might have strong affinity for Cu adsorption. Therotically, the observed distribution of Cu in the current study agrees with metal distribution in coarser fraction in relation to finer fraction of sediments. According to Fig 4.4b, distribution of Cu in acid-soluble phase in coarser fraction is comparatively lower than its distribution in finer fractions. Similar observations were made by Lin et al. (2003). However, Cu concentrations observed in this study are higher than that reported by Lin et al. (2003).

Lead had acid-soluble fraction within the ranges of 0.03 to 49 %. Meanwhile, the exchangeable fractions of Pb in sediment fraction < 63 µm size in other studies were found to be negligible (Wang et al., 2010; Moore et al., 2015). The considerable amount of acid-soluble fraction of Pb in most sampling sites could be attributed to the fraction of Pb bound to carbonate (Moore et al., 2015). The fractions of Pb followed the same distribution pattern in coarser fraction as in finer fraction with slightly lower concentrations (Fig. 4.4c). The result is comparable to the findings of Maslennikova et al. (2012) who reported minimal content (6 % - 20 %) of lead in sediment particle size fractions ranging from 75 - 300 µm.

In the whole sediment fraction, location MO3 recorded the highest (9 %) Fe concentration bound to exchangeable and the carbonate phases. Moreover, only a small fraction (0 - 4 %) of Fe in the < 63 µm particle size of the sediments was found in the exchangeable and carbonate phase at all stations. This phase of Fe bound to carbonate can generally be considered as negligible (Wang et al., 2010; Moore et al., 2015); generally Fe is found in the residual phase (Caplat et al., 2005). Similar distribution of Fe in acid-soluble fraction was observed in the coarser fraction as in finer fraction (Fig 4.4d) and the carbonate bound Fe fraction in the sediment particle size > 63 µm was ≤ 10 % in all stations (Fig 4.4d).

Manganese reported to be weakly bound to the surfaces of carbonate minerals can easily be released through cation exchange processes (Moore et al., 2015). Appendix E; Table E: 5 shows that the exchangeable and carbonate bound manganese accounted for 7 % to 94 % of the total Mn content in the whole sediment fraction. Comparatively, sediment fraction < 63 µm recorded similar but slightly lower Mn fractions bound to the exchangeable and the carbonates in all the sampling sites with concentrations ranging from 6 % - 89 %. However, Mn was mainly found to be bound to the carbonates. The results are in conformity to the findings of other researchers (Sarkar et al., 2014; Moore et al., 2015). Generally, the exchangeable and the carbonate bound Mn in coarser sediments was the dominant phase observed among the four fractions with the exception of sampling site MM4 (Fig 4.4e). The significant amount of Mn bound to carbonate may be remobilized into aquatic environment as Mn-carbonate phase dissociates during acidification (Sarkar et al., 2014).

### **5.2.2. Fraction bound to iron and manganese oxides (Reducible phase, F2)**

Amorphous Iron and Mn oxides have the capacity to adsorb metals and hence greatly regulate mobility and behaviour of metals in sediments (Wang et al., 2010; Moore et al., 2015). The occurrence of Co in reducible phase at site MM4 is considerable in all the sediment fractions (Fig 4.4a). In literature the binding site for Co is reported to be the Fe and Mn oxides (Krupka & Serne, 2002; Howe et al., 2006). Therefore appreciable amount of Co in the reducible phase at location MM4 could be expected since the highest fractions of Fe and Mn in the reducible phases in all the sediment fractions were recorded at MM4 (Appendix E, Table E: 4 and Table E: 5). Appreciable concentrations of Cu, Fe and Mn also occurred in the reducible fraction (Fig 4.4b, Fig 4.4d and Fig 4.4e). The occurrence of Fe and Mn in the reducible fraction is highly expected because the oxides of these elements form the binding sites in this phase. The considerable amount of Cu in the reducible phase in this study supports the findings of Moore et al. (2015) and Tessier et al. (1979). Moreover, Pb adsorption to Fe and Mn oxides was extremely high compared to other binding sites (Fig 4.4c). The highest fraction of Cu and Pb released in the reducible phase suggest that Fe/Mn oxides are the main factors controlling the adsorption, desorption and mobility of these metals under the slightly acidic to neutral pH of the Zambian wetlands. These appreciable amounts of Co and Cu in the reducible phase may be released if the sediments are subjected to intense reducing conditions. This observation confirms the findings made by Sarkar et al. (2014) who found Pb mostly bound to Fe and Mn oxides in sediments. The considerable amount of Pb associated with Fe and Mn oxides can pose serious hazards to the aquatic environments after its release into water column during reduction phase of Fe and Mn oxides in the studied sediments (Sarkar et al., 2014).

### **5.2.3. Fraction bound to organic matter and sulphides (Oxidizable phase, F3)**

With the exception of Cu, relatively low percentages of other selected metals (Co, Pb, Fe and Mn) were found bound to organic matter and sulphides in all sediment fractions. Sediments from stations UM2 and UO2 with the lowest CEC values (Table 4.1) recorded the highest oxidizable phases of Co with significant

negative correlations (Table 4.5). This suggests that, the fraction of Co bound to organic matter and sulphides is unlikely to become mobile as CEC increases. The same sediments had the highest oxidizable fraction of Cu in all the sediment fractions, although both locations recorded relatively very low organic matter content (Table 4.1). This suggests that in these sediments organic matter and sulphides were effective in complexing Co and Cu (Caplat et al., 2005; Sarkar et al., 2014). However, during organic matter degradation and sulphide oxidation, this phase of Co and Cu may be remobilized and pollute the aquatic ecosystem (Wang et al., 2010). Moderate amounts of Cu (20 %, 30 % and 21 %, at MI2) were found binding to oxidizable phase in sediment fraction whole sediment, < 63 µm and > 63 µm respectively. However, compared to the amount (20 %) found in Pasabandor harbour which had only 5.28 % organic matter (Moore et al., 2015), the oxidizable fraction of Cu at MI2 in this study is relatively low in all the sediment fractions. The oxidizable phase of lead at location UO2 was found to be the highest in all sediment fractions compared to other sampling stations (Fig 4.4c). Iron concentration in the oxidizable phase at location MI2 was the highest in all the sediment fractions (Fig 4.4d). This could be attributed to the highest organic matter content at the same location (Table 4.1) since organic matter has strong affinity to complex metals (Peng et al., 2009; Wang et al., 2010). The extremely low amount of Mn found in the oxidizable phase supports the assertion that Mn is not expected to be found bound to organic matter and sulphides (Moore et al., 2015).

#### **5.2.4. Fraction bound to sediment crystalline structure (Residual fraction, F4)**

Metal fractions bound to the crystalline structure of sediments are generally less mobile. About 74 % of total Co concentration has been reported to reside in the residual phase (Sarkar et al., 2014). However, in this current study, approximately 30 - 40 % and 19 - 20 % of Co are respectively concentrated in the inert fraction at locations UM2 and UO2 in all the sediment fractions (Fig. 4.4a). All other stations recorded lower Co concentrations in the residual phase. About 36 % of Cu concentration is associated with the residual fraction in sediments at KI3 in sediment fraction > 63 µm. All other sediment fractions at all locations showed lower Cu concentrations in the residual phase (Fig. 4.4b). The percentage clay proportion and the residual Fe concentration at KI3 were found to be 57 % (Table 4.1) and 97 % (Appendix; Table C: 4) respectively. The relatively high clay content and residual Fe in sediments from KI3 were capable in scavenging Cu from solution and incorporated it in the crystalline structure of the sediments. Sarkar et al. (2014) reported that, Cu easily chemisorbed in clay minerals. The geochemical phase of Pb in the residual phase was found to be about 30 % at location MI2 in the sediment fraction > 63 µm size (Fig. 4.3c). Other sediments from the remaining sampling sites recorded lower than 20 % Pb concentration in the residual phase, suggesting that greater proportion of Pb occurred in the mobile fractions in those sediments. This is an indication that Pb can pose a major risk to the aquatic living resources in the wetlands containing such sediments. Similar observation has been reported by Sarkar et al. (2014). The major geochemical phase of Fe was found in the residual fraction at all stations in all sediment fractions (Fig 4.4d). This confirms the popular knowledge on binding site for Fe in sediments (Caplat et al., 2005). Comparatively, Mn recorded minimal content in the residual phase and at MM4 its content could be described as negligible in all sediment fractions (Fig 4.4e).

### 5.2.5. Correlation study

Using the entire data set obtained from the study, significant correlations ( $= 0.05, 0.01$ ) were recorded between some fractions of the metals and the sediment pH, EC and CEC. Negative significant correlations were observed between most fractions of Co and Cu investigated in all the three different sediment fractions with sediment CEC. This phenomenon is of great concern as increase levels of these metals may result in significant reduction in essential minerals such as  $\text{Ca}^{2+}$ ,  $\text{Mg}^{2+}$  which are required by the aquatic living resources for metabolic processes. This finding is comparable to the findings of Ololade et al. (2008) who found similar results in Ondo coastal sediment in Nigeria. On the other hand, it was observed that the oxidizable fraction of lead correlated positively with CEC in the whole sediment fraction while in other sediment fractions no significant correlation was found between Pb and CEC. This is an indication that Pb pollution may increase in the whole sediment fraction as CEC increases. However, the negative correlation observed between fractions of Co and Cu may be attributed to cation selectivity phenomenon. Both Co and Cu compete with other cations for exchange sites. Therefore, as CEC increases, other cations such as Zn, Pb, etc. with higher selectivity coefficient relative to Co and Cu will have a competitive advantage to be adsorbed onto the exchange sites and vice versa (Appel et al., 2003). Also, the negative correlation may be in connection with the highest concentrations of Pb found in KI3 and KO1 relative to Co and Cu (Appendix C, Table C: 1). This may have caused increase concentrations of Co and Cu as CEC increase to be seemingly negligible because exchange sites may be entirely occurred by Pb.

The lack of correlation found between moisture, pH, organic matter, EC and fractions of Co and Cu in all the sediment fractions shows that Co and Cu are sourced differently from these sediment characteristics. However, the positive linear correlation between F1 fraction of Mn and organic indicates that organic matter may play a role significant role in regulating the most mobile fraction of Mn. Increase moisture in the sediment may potentially cause dissociation of the reducible phase of Fe as moisture showed significant correlation with some fractions of Fe. With the exception of the acid-soluble fraction of Pb, all other fractions correlated negatively with sediment pH in all the three different sediment fractions, a phenomenon which may increase Pb mobility in the wetland environment. Surprisingly, only the fraction of Co bound to Fe and Mn oxides recorded positive correlation with temperature indicating that increase temperature is likely capable of remobilizing the reducible phase of Co in the sediments. The electrical conductivity of the sediments correlated positively with all the phases of Pb in the sediment fractions  $< 63 \mu\text{m}$  and  $> 63 \mu\text{m}$  sizes (Table 4.5). However, with the exception of fractions F1 and F3, the remaining fractions; F2, mobile fraction and the total Pb concentrations in the whole sediments correlated positively with EC. This shows that increase EC may increase the mobile phases of Pb in the sediments and consequently increase the ability of the sediments to conduct electricity. Electrical conductivity is therefore the main regulator of Pb in the studied sediment. These findings confirm the findings of Ravichandran (2014). With the exception of acid-soluble phase (F1) of Mn showing positive correlation with organic matter sediment fraction  $> 63 \mu\text{m}$ , all other fractions and the fraction of Fe did not correlate with sediment physicochemical characteristics. Based on the findings of this current study, EC was found to be the dominant sediment characteristic over metal bonds while CEC and pH played a significant role in metal mobility in the sediments.

### 5.2.6. Potential metal mobility assessment

Of all the elements studied, Mn has the highest mobility in sediment particle-size fraction  $< 63 \mu\text{m}$ , since it presents the highest content in the acid-soluble (most labile) phase. This is particularly marked in all the sampling sites except MM4 where Mn associated with the F1 fraction reaches levels of more than 50 % of the total content (Fig 4.5b). In the sediment fraction  $< 63 \mu\text{m}$ , Mn seemed to be the most mobile elements.

Approximately, 50 - 80 % of its total concentration was measured in the first extraction, and about 20 - 50 % of which were found in the second fraction. The very high risk levels of Mn in the sediment fractions may be attributed to the mobile nature of Mn in sediments (Alhashemi et al., 2013; Moore et al., 2015). This distribution of Mn in particle-size < 63  $\mu\text{m}$  is not unusual, since Mn has been found to be of extreme risk for the environment in other studies (Sungur et al., 2014). The very low amount of Fe in the acid-soluble phase as a percentage of the total concentration limits the potential toxicity capacity of Fe. Fe and Mn are essentially not-toxic to living organisms because they are needed for metabolic processes. However, concentrations above threshold levels can be detrimental to aquatic life. The potential toxicity of Co and Cu was more pronounced in the sediment fraction < 63  $\mu\text{m}$  size compared to other particle sizes, with most sampling sites recording very high risk and high risk levels of Co and Cu respectively (Fig 4.5b). This can be attributed to the presence of large surface area of particle size < 63  $\mu\text{m}$  in accumulating metals (John & Leventhal, 1995). Lead on the other hand posed very high risk, high risk and medium risk for the environments in all the particle size fractions but the effects was comparatively less pronounced (Fig. 4.5a, Fig 4.5b and Fig. 4.5c). However, it should be pointed out that, the mobility of the elements from the sediments does not necessarily indicate their bioavailable to aquatic living resources due to the ability of other sediment binding sites forming complexes with the mobile fractions.

### **5.2.7. Assessment of potential toxicity using Canadian Sediment Quality Guidelines (SQG)**

In sediment fraction < 63  $\mu\text{m}$  size, the concentrations of Cu exceeded the PEL values in all the sampling locations (Table 4.4), indicating that toxicity effect of Cu to the aquatic biota is probable. Concentrations of Pb were also higher than PEL at sampling sites KI3, KO1 and UM2 and therefore above the threshold at which adverse effect on organisms in the wetlands can be predicted. However, Pb concentrations at the remaining sampling sites were higher than TEL but lower than PEL and therefore toxicity effect of Pb on organisms at these sites was uncertain. Toxicity of Cu in the coarser fraction is comparable to its toxicity in the finer fraction (Table 4.4). With the exception of sediments from location KI3, concentrations of Cu at the remaining sampling sites exceeded the PEL values, suggesting that the wetland environments were not only polluted with Cu but the adverse effect of this metal on aquatic organisms can be expected. Location KI3 had Cu concentration higher than the TEL but lower than PEL values, indicating that evaluation of Cu toxicity on biota at sampling site (KI3) can not be reliably predicted. Toxicity effect of Pb can be predicted at locations KI3 and KO1 in sediment fraction > 63  $\mu\text{m}$  size (Table 4.4). However, the concentrations of Pb at the remaining sampling sites were below than TEL value, indicating that toxic effects on organisms in the studied wetlands were unlikely to occur. Similar toxicity effect of Cu was observed in the whole sediment fraction as observed in the finer fraction with all the sampling sites recording concentrations higher than the PEL values (Table 4.4). This suggests that, the studied wetlands are highly contaminated with Cu and that aquatic living resources may be adversely affected by the toxicity effect of Cu.

Concentrations of Pb at sampling locations KI3 and KO1 in whole sediment fraction exceeded the PEL, indicating adverse effect of Pb on aquatic organisms at those particular wetland environments. However, Pb concentrations at locations UM2 and UO2 were higher than TEL but lower than PEL, suggesting that adverse effect of Pb on organisms at these locations can not accurately be predicted. Toxic effects of Pb in the whole sediment fraction at the remaining locations are unlikely to occur. However, it should be noted that, the biogeochemical characteristics of the environment for which the threshold levels enshrined in the Canadian (SQG) were developed may be entirely different from the biogeochemical properties of the current study area (Santos et al., 2013), therefore the results must be interpreted with caution.

## CHAPTER 6

# Conclusions and Recommendations

---

## 6.1. Conclusions

- In this study on Zambian wetland sediment, metal partitioning of the sediment analyses revealed that, Co, Cu and Mn were mainly bound to the exchangeable and carbonate binding sites while lower concentrations resided in the residual phase. Pb was mainly concentrated in the reducible phase while Fe principally resided in the residual fraction.
- Metal distribution of the studied sediments followed different patterns in the respective particle-size fractions at each location. However, particle-size < 63 µm recorded comparatively higher metals than both the whole sediment and the coarser fractions. The whole sediments showed an average behaviour on metal distribution.
- The risk assessment code (RAC) revealed potential mobility and toxicity of the metals in the studied wetlands with the exception of Fe. Mobility of the metals is likely to be more pronounced in the finer fraction than the remaining fractions.
- Significant correlations between EC, CEC, pH and most fractions of the metals indicate that these sediment characteristics may control the fate and transport of the metals in the sediments.

## 6.2. Recommendations

- Based on the findings of this study, the BCR method when used for metal determinations has the possibility of contamination resulting from preceding steps and this can conceal the actual metal concentrations in the sediments. Results from BCR-SEP in this study must therefore be interpreted with caution.
- Further studies may consider the determination of carbonate and sulphide contents in the sediments. This will unravel the reasons why highest fraction of Co is bound to exchangeable and the carbonate binding sites and considerable amount of Cu associated with the oxidizable phase even though organic matter did not show significant correlation with fractions of Cu
- Due to the high levels of metal concentrations (above the PEL) observed in this study, further investigation is recommended for heavy metal toxicity study.

# References

- Adiyiah, J., Kelderman, P. 2014. Assessment of the Levels of Heavy Metals in Vertical Sediment Cores of Lake Markermeer in the Netherlands. *International Journal of Engineering Research and Technology*. ESRSA Publications.
- Akhurst, D.J., Clark, M.W., Reichelt-Brushett, A., Jones, G.B. 2011. Grain size normalization: a case for post extraction normalization and inclusion of selective extraction procedures. *Limnology and Oceanography: Methods*, **9**(5), 215-231.
- Alhashemi, A.H., Karbassi, A.R., Kiabi, B.H., Monavari, S.M., Nabavi, M.B. 2013. Accumulation and bioaccessibility of trace elements in wetland sediments. *African Journal of Biotechnology*, **10**(9), 1625-1636.
- Appel, C., Ma, L.Q., Rhue, R.D., Reve, W. 2003. Selectivities of potassium-calcium and potassium-lead exchange in two tropical soils. *Soil Science Society of America Journal*, **67**(6), 1707-1714.
- Balintova, M., Petrilkova, A., Singovszka, E. 2012. Study of metals distribution between water and sediment in the Smolnik creek (Slovakia) contaminated by acid mine drainage. *Chemical Engineering*, **28**.
- Bragato, C., Brix, H., Malagoli, M. 2006. Accumulation of nutrients and heavy metals in *Phragmites australis* (Cav.) Trin. ex Steudel and *Bolboschoenus maritimus* (L.) Palla in a constructed wetland of the Venice lagoon watershed. *Environmental Pollution*, **144**(3), 967-975.
- Callender, E. 2003. Heavy metals in the environment-historical trends. *Treatise on geochemistry*, **9**, 67-105.
- Caplat, C., Texier, H., Barillier, D., Lelievre, C. 2005. Heavy metals mobility in harbour contaminated sediments: the case of Port-en-Bessin. *Mar Pollut Bull*, **50**(5), 504-11.
- Copaja, S.V., Molina, X., Tessada, R. 2014. Determination of heavy metals in Choapa River sediments using BCR sequential extraction procedure. *Journal of the Chilean Chemical Society*, **59**(1), 2353-2358.
- Cynthia, L., Fianko, J., Akiti, T., Osei, J., Brimah, A., Osae, S., Bam, E. 2011. Determination of trace elements in the Sakumo wetland sediments.
- Day, D., Beyer, W., Hoffman, D., Morton, A., Sileo, L., Audet, D., Ottinger, M. 2003. Toxicity of lead-contaminated sediment to mute swans. *Archives of environmental contamination and toxicology*, **44**(4), 0510-0522.
- Fernandez, E., Jimenez, R., Lallena, A.M., Aguilar, J. 2004. Evaluation of the BCR sequential extraction procedure applied for two unpolluted Spanish soils. *Environ Pollut*, **131**(3), 355-64.
- Filgueiras, A.V., Lavilla, I., Bendicho, C. 2002. Chemical sequential extraction for metal partitioning in environmental solid samples. *Journal of Environmental Monitoring*, **4**(6), 823-857.
- Förstner, U. 2004. Traceability of sediment analysis. *TrAC Trends in Analytical Chemistry*, **23**(3), 217-236.
- Guagliardi, I., Apollaro, C., Scarciglia, F., De Rosa, R. 2013. Influence of particle-size on geochemical distribution of stream sediments in the Lese river catchment, southern Italy. *Base*.
- Guevara-Riba, A., Sahuquillo, A., Rubio, R., Rauret, G. 2004. Assessment of metal mobility in dredged harbour sediments from Barcelona, Spain. *Sci Total Environ*, **321**(1-3), 241-55.
- Horowitz, A.J. 1985. *A primer on trace metal-sediment chemistry*. US Government Printing Office.
- Howe, M.P.D., Wood, M., Huntingdon, C. 2006. Cobalt and inorganic cobalt compounds.
- Idriss, A.A., Ahmad, A.K. 2013. Heavy Metals Nickel and Chromium in Sediments in the Juru River, Penang, Malaysia. *Journal of Environmental Protection*, **04**(11), 1245-1250.
- Ikenaka, Y., Nakayama, S.M., Muzandu, K., Choongo, K., Teraoka, H., Mizuno, N., Ishizuka, M. 2010. Heavy metal contamination of soil and sediment in Zambia. *African Journal of Environmental Science and Technology*, **4**(11), 729-739.
- Imhansoloeva, T.M., Akintoye, A.E., Mayowa, I.P., Abdulkarim, R., Oguwuike, I.D., Olubukola, S., Ruth, F.B. 2011. Numerical assessment and analysis of textural deposits of beach sediment: A case study of Ajah (Okun Mopo) Beach Lagos South West Nigeria. *Nature and Science*, **9**(8), 165-174.
- Jain, C.K., Gupta, H., Chakrapani, G.J. 2008. Enrichment and fractionation of heavy metals in bed sediments of River Narmada, India. *Environ Monit Assess*, **141**(1-3), 35-47.
- John, D.A., Leventhal, J.S. 1995. Bioavailability of metals. *Preliminary compilation of descriptive geoenvironmental mineral deposit models*, 10-18.

- Kabala, C., Karczewska, A., Szopka, K., Wilk, J. 2011. Copper, zinc, and lead fractions in soils long-term irrigated with municipal wastewater. *Communications in soil science and plant analysis*, **42**(8), 905-919.
- Kamona, A., Friedrich, G. 2007. Geology, mineralogy and stable isotope geochemistry of the Kabwe carbonate-hosted Pb–Zn deposit, Central Zambia. *Ore Geology Reviews*, **30**(3), 217-243.
- Kartal, S., Birol, G. 2003. Application of a Three-Stage Sequential Extraction Procedure for the Determination of Extractable Metal. *Turk J Chem*, **27**, 333-346.
- Kelderman, P., Osman, A. 2007. Effect of redox potential on heavy metal binding forms in polluted canal sediments in Delft (The Netherlands). *Water research*, **41**(18), 4251-4261.
- Kersten, M., Förstner, U. 1986. Chemical fractionation of heavy metals in anoxic estuarine and coastal sediments. *Water Science & Technology*, **18**(4-5), 121-130.
- Křibek, B., Majer, V., Veselovský, F., Nyambe, I. 2010. Discrimination of lithogenic and anthropogenic sources of metals and sulphur in soils of the central-northern part of the Zambian Copperbelt Mining District: a topsoil vs. subsurface soil concept. *Journal of Geochemical Exploration*, **104**(3), 69-86.
- Kruis, F. 2007. Environmental Chemistry; selected methods for water quality Analysis, Laboratory Manual. LN0168/07/1, UNESCO-IHE, The Netherlands.
- Krupka, K., Serne, R. 2002. Geochemical factors affecting the behavior of antimony, cobalt, europium, technetium, and uranium in vadose sediments. *Report PNNL*, **14126**.
- Liddle, E.S., Mager, S.M., Nel, E. 2014. Water quality awareness and barriers to safe water provisioning in informal communities: A case study from Ndola, Zambia. *Bulletin of Geography. Socio-economic Series*, **26**(26), 167-181.
- Lin, J.-G., Chen, S.-Y. 1998. The relationship between adsorption of heavy metal and organic matter in river sediments. *Environment International*, **24**(3), 345-352.
- Lin, J., Chen, S., Su, C. 2003. Assessment of sediment toxicity by metal speciation in different particle-size fractions of river sediment. *Water Science & Technology*, **47**(7), 233-241.
- Ma, L., Xu, R., Jiang, J. 2010. Adsorption and desorption of Cu (II) and Pb (II) in paddy soils cultivated for various years in the subtropical China. *Journal of Environmental Sciences*, **22**(5), 689-695.
- Maslennikova, S., Larina, N., Larin, S. 2012. The Effect of Sediment Grain Size on Heavy Metal Content. *Lakes, Reservoirs and Ponds*, **6**(1), 43-54.
- Moore, F., Nematollahi, M.J., Keshavarzi, B. 2015. Heavy metals fractionation in surface sediments of Gowatr bay–Iran. *Environ Monit Assess*, **187**(1), 4117.
- Morillo, J., Usero, J., Gracia, I. 2004. Heavy metal distribution in marine sediments from the southwest coast of Spain. *Chemosphere*, **55**(3), 431-42.
- Nematollahi, M.J.E., M. 2015. Investigation of Heavy Metals Origin in Surface Sediments of Gowatr Bay, SE Iran Using Geostatistical Analyses. *Geochemistry Journal*, **2**(1).
- Ogunfowokan, A., Oyekunle, J., Olutona, G., Atoyebi, A., Lawal, A. 2013. Speciation Study of Heavy Metals in Water and Sediments from Asunle River of the Obafemi Awolowo University, Ile-Ife, Nigeria. *International Journal of Environmental Protection*.
- Okoro, H.K., Fatoki, O.S. 2012. A Review of Sequential Extraction Procedures for Heavy Metals Speciation in Soil and Sediments. *Journal of Environmental & Analytical Toxicology*, **01**(S1).
- Ololade, I., Lajide, L., Amoo, I. 2008. Seasonal metal distribution in Ondo coastal sediment, Nigeria. *Journal of Applied Sciences and Environmental Management*, **12**(4).
- Pam, A.A., Sha’Ato, R., Offem, J.O. 2013. Evaluation of heavy metals in soils around auto mechanic workshop clusters in Gboko and Makurdi, Central Nigeria. *Journal of Environmental Chemistry and Ecotoxicology*, **5**(11), 298-306.
- Parizanganeh, A. 2008. Grain size effect on trace metals in contaminated sediments along the Iranian coast of the Caspian Sea. *Proceedings of Taal2007: The 12th World Lake Conference*. pp. 336.
- Peng, J.F., Song, Y.H., Yuan, P., Cui, X.Y., Qiu, G.L. 2009. The remediation of heavy metals contaminated sediment. *J Hazard Mater*, **161**(2-3), 633-40.
- Prasanth, K., Sreekala, P., Sandeep, S., Kripa, P., Sreejesh, K. 2013. Heavy Metals and its Fractions in Soils of Koratty Region, Kerala. *Research Journal of Recent Sciences* **2277**, 2502.
- Puttaiah, E.T., Kiran, B.R. 2007. Heavy metal transport in a sewage fed lake of Karnataka, India. *Proceedings of Taal. The 12th world lake conference*. pp. 347-354.

- Quevauviller, P., Rauret, G., López-Sánchez, J.-F., Rubio, R., Ure, A., Muntau, H. 1997. Certification of trace metal extractable contents in a sediment reference material (CRM 601) following a three-step sequential extraction procedure. *Science of the Total Environment*, **205**(2), 223-234.
- Santos, I.S., Garcia, C.A., Passos, E.A., Alves, J.P. 2013. Distributions of trace metals in sediment cores from a hypertrophic reservoir in northeast Brazil. *Journal of the Brazilian Chemical Society*, **24**(2), 246-255.
- Sarkar, S.K., Favas, P.J., Rakshit, D., Satpathy, K. 2014. Geochemical Speciation and Risk Assessment of Heavy Metals in Soils and Sediments.
- Sekomo, C.B., Nkuranga, E., Rousseau, D.P., Lens, P.N. 2011. Fate of heavy metals in an urban natural wetland: The Nyabugogo swamp (Rwanda). *Water, Air, & Soil Pollution*, **214**(1-4), 321-333.
- Shetye, S.S., Sudhakar, M., Mohan, R., Tyagi, A. 2009. Implications of organic carbon, trace elemental and CaCO<sub>3</sub> variations in a sediment core from the Arabian Sea. *Indian J Mar Sci*, **384**(4), 432-438.
- Silva, G.S.d., Nascimento, A.S.d., Sousa, E.R.d., Marques, E.P., Marques, A.L.B., Corrêa, L.B., Silva, G.S.d. 2014. Distribution and Fractionation of Metals in Mangrove Sediment from the Tibiri River Estuary on Maranhão Island. *Revista Virtual de Química*, **6**(2).
- Silveira, M., Alleoni, L., O'connor, G., Chang, A. 2006. Heavy metal sequential extraction methods—a modification for tropical soils. *Chemosphere*, **64**(11), 1929-1938.
- Singh, A.K., Hasnain, S., Banerjee, D. 1999. Grain size and geochemical partitioning of heavy metals in sediments of the Damodar River—a tributary of the lower Ganga, India. *Environmental geology*, **39**(1), 90-98.
- Sposito, G., Lund, L., Chang, A. 1982. Trace metal chemistry in arid-zone field soils amended with sewage sludge: I. Fractionation of Ni, Cu, Zn, Cd, and Pb in solid phases. *Soil Science Society of America Journal*, **46**(2), 260-264.
- Sracek, O., Křibek, B., Mihaljevič, M., Majer, V., Veselovský, F., Vencelides, Z., Nyambe, I. 2012. Mining-related contamination of surface water and sediments of the Kafue River drainage system in the Copperbelt district, Zambia: an example of a high neutralization capacity system. *Journal of Geochemical Exploration*, **112**, 174-188.
- Sungur, A., Soylak, M., Yilmaz, S., Özcan, H. 2014. Determination of heavy metals in sediments of the Ergene River by BCR sequential extraction method. *Environmental Earth Sciences*, **72**(9), 3293-3305.
- Sutherland, R.A., Tack, F.M., Ziegler, A.D. 2012. Road-deposited sediments in an urban environment: A first look at sequentially extracted element loads in grain size fractions. *Journal of hazardous materials*, **225**, 54-62.
- Tessier, A., Campbell, P. 1987. Partitioning of trace metals in sediments: relationships with bioavailability. *Hydrobiologia*, **149**(1), 43-52.
- Tessier, A., Campbell, P.G., Bisson, M. 1979. Sequential extraction procedure for the speciation of particulate trace metals. *Analytical chemistry*, **51**(7), 844-851.
- Ure, A., Davidson, C. 2002. Chemical speciation in soils and related materials by selective chemical extraction. *Chemical Speciation in the Environment, Second Edition*, 265-300.
- Wang, S., Jia, Y., Wang, S., Wang, X., Wang, H., Zhao, Z., Liu, B. 2010. Fractionation of heavy metals in shallow marine sediments from Jinzhou Bay, China. *Journal of Environmental Sciences*, **22**(1), 23-31.
- Wright, D.A., Welbourn, P. 2002. *Environmental toxicology*. Cambridge University Press.
- Zerbe, J., Sobczynski, T., Elbanowska, H., Siepak, J. 1999. Speciation of heavy metals in bottom sediments of lakes. *Polish Journal of Environmental Studies*, **8**, 331-340.
- Zhao, H., Li, X., Wang, X., Tian, D. 2010. Grain size distribution of road-deposited sediment and its contribution to heavy metal pollution in urban runoff in Beijing, China. *Journal of hazardous materials*, **183**(1), 203-210.

# Appendices

## Appendix A Wet sieving analytical data for particle size determination and the corresponding percentages of sediment particle size fractions

Table A.1 Results of the grain-size analysis for the studied sediments

Site	Sieve size (mm)	Weight retained (g)	Weight retained (%)	Cumulative retained (%)	Finer (%)
KI3	2	4.47	-	-	-
	1	2.99	6.6	6.6	93.4
	0.5	3.05	6.7	13.3	86.7
	0.25	4.18	9.2	22.5	77.5
	0.125	4.46	9.8	32.3	67.7
	0.063	4.72	10.4	42.7	57.3
	<0.063	26.0	57.3	100	0
KO1	2	1.0	-	-	-
	1	2.38	5.0	5.0	95.0
	0.5	2.05	4.3	9.3	90.7
	0.25	2	4.2	13.6	86.4
	0.125	3.52	7.4	21.0	79.0
	0.063	5.4	11.4	32.4	67.6
	<0.063	32.1	67.6	100	0
MI2	2	0.02	-	-	-
	1	0.1	0.3	0.3	99.7
	0.5	0.52	1.4	1.7	98.3
	0.25	1.22	3.4	5.1	94.9
	0.125	4.23	11.8	16.9	83.1
	0.063	11.3	31.5	48.3	51.7
	0.01	18.6	51.7	99.7	0
MM4	2	0.05	-	-	-
	1	0.25	0.5	0.5	99.5
	0.5	0.75	1.5	2.0	98.0
	0.25	5.25	10.5	12.5	87.5
	0.125	14.1	28.3	40.8	59.2
	0.063	10.0	20.1	60.9	39.1
	<0.063	19.5	39.1	100	0

Table A: 1 (Cont...)

Table A:1 (Continuation): Results of the grain-size analysis for the studied sediments

Site	Sieve size (mm)	weight retained (g)	Weight retained (%)	Cumulative retained (%)	Finer (%)
MO3	2	2.19	-	-	-
	1	1.85	3.9	3.9	96.1
	0.5	0.85	1.8	5.7	94.4
	0.25	1.70	3.6	9.2	90.8
	0.125	9.19	19.2	28.4	71.6
	0.063	9.64	20.9	48.6	51.4
	0.01	24.5	51.4	100	0
UM2	2	0.06	-	-	-
	1	0.11	0.2	0.2	99.8
	0.5	0.35	0.7	0.9	99.1
	0.25	4.33	8.7	9.6	90.4
	0.125	16.8	33.7	43.3	56.7
	0.063	14.4	28.9	72.3	27.7
	<0.063	13.8	27.7	100	0
UO2	2	0.00	-	-	-
	1	0.12	0.3	0.3	99.8
	0.5	0.47	1.0	1.2	98.8
	0.25	1.00	2.1	3.3	96.7
	0.125	11.1	23.0	26.3	73.7
	0.063	16.4	34.0	60.4	39.6
	<0.063	19.1	39.6	100	0

# Appendices

Appendix B : Data related to the measurement of physico-chemical characteristics of the studied sediments.

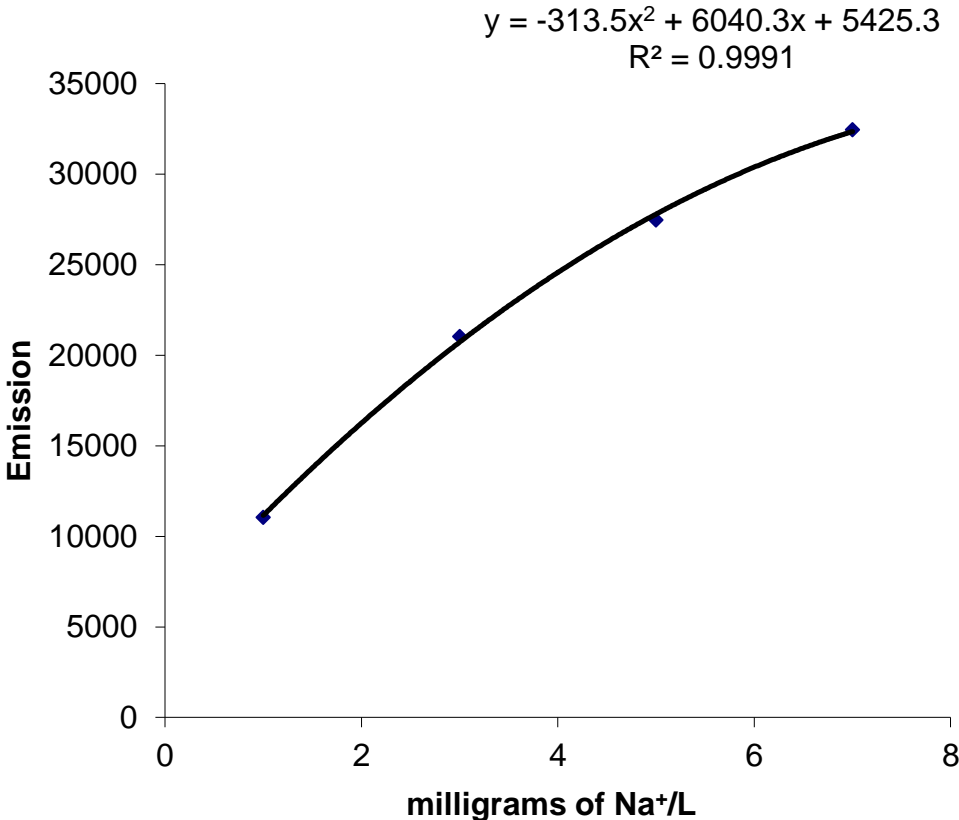


Figure B.1 Cation exchange capacity (CEC) calibration curves for the selected sediment samples

## Appendix C Microwave-assisted digestion analytical data for total metal

### concentrations in different sediment particle-size distribution

Table C.1 Results of total metals concentrations (mean±SD, mg kg<sup>-1</sup>) in the respective sediment fractions (Laboratory replicates, n = 3)

Particle size	Site	Elements				
		Co	Cu	Pb	Fe	Mn
Whole sediments	KI3	160±0.5	500±6.0	6300±145.1	37000±1889.5	2000±39.6
	KO1	400±6.5	2900±39.6	43000±474.7	4900±999.9	3900±183.5
	MI2	250±2.6	2800±39.7	10±0.6	19000±337.8	7200±134.3
	MM4	260±10.3	1400±47.4	30±1.0	23000±182.1	13000±525.1
	MO3	130±0.7	1600±1.1	30±0.9	25000±791.6	3800±35.2
	UM2	1000±25.0	11000±76.5	60±10.9	28000±1163.4	800±6.5
	UO2	1500±2.4	9600±46.6	50±1.4	28000±822.8	1800±13.18
Fraction < 63 µm	KI3	170±6.9	710±24.8	7600±198.7	32000±1811	1600±71.9
	KO1	320±3.5	3400±52.7	38000±214.4	56000±1192	1800±4.0
	MI2	280±7.0	3600.7±82.1	40±0.9	25000±540.4	7600±79.5
	MM4	400±26.2	2200±160.2	60±5.1	42000±3011	19000±1232
	MO3	130±3.9	2300±58.6	50±1.2	33000±358.2	2900±9.5
	UM2	2400±39.3	28000±678.4	140±0.8	52000±742.1	1100±9.7
	UO2	2100±42.5	17000±261.6	90±1.5	43000±709.5	1800±13.2
Fraction > 63 µm	KI3	40±0.7	100±2.4	4800±61.8	52000±512.2	3100±139.4
	KO1	240±4.0	1800±17	46000±822.9	44000±409.4	5700±442.1
	MI2	210±6.5	2200±37.6	10±0.7	14100±377.9	6000±30.8
	MM4	220±0.3	930±31.8	10±0.7	9400±412.1	11000±26.4
	MO3	60±1.1	830±8.0	20±0.6	9800±315.0	2400±62.4
	UM2	500±8.6	5500±392	30±6.1	19000±135.6	700±15.4
	UO2	850±16.1	4200±66	10±0.9	18000±366.1	1600±19.54

**Appendix D Mass balance of total metal concentration in difference sediment particle-size fractions**

Table D.1: Mass balance of total metal concentrations in three sediment particle-size fractions (Laboratory replicates, n = 3)

Metal	Site	Particle-size		Total metal concentration (mean±SD, mg kg <sup>-1</sup> )			Mass balance (%)	Mass balance (%)
		Finer (%) (<63 µm)	Sand (%) (>63 µm)	Fraction < 63 µm	Fraction > 63 µm	Whole sediment		
Co	KI3	0.57	0.43	170±6.9	40±0.7	160±0.5	110	71
	KO1	0.68	0.32	320±3.5	240±4.0	400±6.5	300	73
	MI2	0.52	0.48	280±7.0	210±6.5	250±2.6	250	97
	MM	0.39	0.61	400±26.2	220±0.3	260±10.3	289	110
	MO3	0.51	0.49	130±3.9	60±1.1	130±0.7	100	74
	UM2	0.28	0.72	2400±39.3	500±8.6	1000±25.0	1000	103
	UO2	0.4	0.6	2100±42.5	850±16.1	1500±2.4	1400	93
Cu	KI3	0.57	0.43	710±24.8	100±2.4	500±6.0	440	90
	KO1	0.68	0.32	3400±52.7	1800±17	2900±39.6	2900	102
	MI2	0.52	0.48	3600.7±82.1	2200±37.6	2800±39.7	2900	104
	MM4	0.39	0.61	2200±160.2	930±31.8	1400±47.4	1400	105
	MO3	0.51	0.49	2300±58.6	830±8.0	1600±1.1	1600	96
	UM2	0.28	0.72	28000±678.4	5500±392	11000±76.5	12000	106
	UO2	0.4	0.6	17000±261.6	4200±66	9600±46.6	9200	96
Pb	KI3	0.57	0.43	7600±198.7	4800±61.8	6300±145.1	6400	102
	KO1	0.68	0.32	38000±214.4	46000±822.9	43000±474.7	41000	95
	MI2	0.52	0.48	40±0.9	10±0.7	10±0.6	30	180
	MM4	0.39	0.61	60±5.1	10±0.7	30±1.0	30	110
	MO3	0.51	0.49	50±1.2	20±0.6	30±0.9	40	123
	UM2	0.28	0.72	140±0.8	30±6.1	60±10.9	60	100
	UO2	0.4	0.6	90±1.5	10±0.9	50±1.4	50	99

Table D:1 (Cont...)

Table D:1 (Continuation): Mass balance of total metal concentrations in three sediment particle-size fractions (Laboratory replicates, n = 3)

Metal	Site	Particle-size		Total metal concentration (mean±SD, mg kg <sup>-1</sup> )			Mass balance	Mass balance (%)
		Finer (%) (<63 µm)	Sand (%) (>63 µm)	Fraction < 63 µm	Fraction > 63 µm	Whole sediment		
Fe	KI3	0.57	0.43	32000±1811	52000±512.2	37000±1889.5	41000	109
	KO1	0.68	0.32	56000±1192	44000±409.4	4900±999.9	52000	108
	MI2	0.52	0.48	25000±540.4	14100±377.9	19000±337.8	20000	105
	MM4	0.39	0.61	42000±3011	9400±412.1	23000±182.1	22000	96
	MO3	0.51	0.49	33000±358.2	9800±315.0	25000±791.6	22000	88
	UM2	0.28	0.72	52000±742.1	19000±135.6	28000±1163.4	28000	102
	UO2	0.4	0.6	43000±709.5	18000±366.1	28000±822.8	28000	100
Mn	KI3	0.57	0.43	1600±71.9	3100±139.4	2000±39.6	2200	109
	KO1	0.68	0.32	1800±4.0	5700±442.1	3900±183.5	3000	77.8
	MI2	0.52	0.48	7600±79.5	6000±30.8	7200±134.3	6900	95
	MM4	0.39	0.61	19000±1232	11000±26.4	13000±525.1	14000	113
	MO3	0.51	0.49	2900±9.5	2400±62.4	3800±35.2	2700	71
	UM2	0.28	0.72	1100±9.7	700±15.4	800±6.5	820	109
	UO2	0.4	0.6	1800±13.2	1600±19.54	1800±13.18	1700	93

S.D = Standard deviation

**Appendix E BCR-SEP analytical data for metal fractions in different sediment particle size distribution**

Table E.1 Distribution of cobalt (Co) under the four binding sites in different particle-size fractions

Particle size	Sites	Metal concentration (%)			
		F1	F2	F3	F4
Less than 63 $\mu\text{m}$ size fraction	KI3	69.7	15.0	12.9	2.4
	KO1	68.7	18.6	10.0	2.5
	MI2	64.0	16.5	15.6	3.9
	MM4	0.6	96.5	1.4	1.5
	MO3	59.2	21.2	12.8	6.8
	UM2	29.3	15.6	22.4	32.8
	UO2	42.5	16.4	19.1	22.0
Greater than 63 $\mu\text{m}$ size fraction	KI3	69.4	15.0	7.5	8.1
	KO1	59.0	32.8	6.2	2.0
	MI2	68.3	18.3	10.9	2.5
	MM4	0.9	98.0	0.40	0.7
	MO3	67.4	18.0	12.2	2.5
	UM2	29.7	14.7	15.6	40.1
	UO2	49.1	14.5	17.7	18.7
Whole sediments fraction	KI3	72.2	10.5	14.4	2.9
	KO1	82.8	9.8	6.2	1.2
	MI2	68.1	12.7	16.8	2.4
	MM4	1.1	96.4	1.2	1.4
	MO3	48.8	12.2	35.2	3.8
	UM2	29.5	12.5	20.5	37.5
	UO2	47.1	13.6	17.1	22.2

Table E.2 Distribution of copper (Cu) under the four binding sites in different particle size fractions (Laboratory replicates, n = 2)

Particle size	Sites	Metal concentration (%)			
		F1	F2	F3	F4
Less than 63 $\mu\text{m}$ size fraction	KI3	25.4	44.4	21.4	8.9
	KO1	34.8	49.6	13.3	2.4
	MI2	49.1	27.5	21.3	2.1
	MM4	28.1	57.2	9.20	5.4
	MO3	43.8	33.4	18.6	4.2
	UM2	38.3	12.3	41.9	7.6
	UO2	32.7	13.5	47.4	6.5
Greater than 63 $\mu\text{m}$ size fraction	KI3	15.3	32.0	16.2	36.4
	KO1	19.2	59.3	18.6	2.9
	MI2	38.3	29.2	30.4	2.1
	MM4	29.3	56.3	10.7	3.8
	MO3	26.9	34.1	34.3	4.7
	UM2	20.1	11.3	52.1	16.4
	UO2	14.8	18.6	61.2	5.3
Whole sediments fraction	KI3	6.80	51.0	33.2	8.92
	KO1	13.3	61.3	23.0	2.38
	MI2	56.8	21.5	20.2	1.55
	MM4	33.7	52.0	10.0	4.3
	MO3	38.2	30.9	27.6	3.4
	UM2	32.8	12.8	45.2	9.2
	UO2	23.3	13.9	55.3	7.5

Table E.3 Distribution of lead (Pb) under the four binding sites in different particle size fractions (Laboratory replicates, n = 2)

Particle size	Site	Metal concentration (%)			
		F1	F2	F3	F4
Less than 63 $\mu\text{m}$ size	KI3	49.5	44.7	2.1	3.70
	KO1	41.6	52.6	4.0	1.80
	MI2	6.0	81.2	0.0	12.8
	MM4	0.0	83.8	2.8	13.4
	MO3	4.6	75.7	5.0	14.7
	UM2	24.2	60.3	3.9	11.6
	UO2	17.5	63.6	6.3	12.6
Greater than 63 $\mu\text{m}$ size	KI3	50.7	38.2	3.4	7.7
	KO1	18.2	77.8	2.6	1.4
	MI2	2.0	64.6	3.4	30.0
	MM4	0.3	86.2	2.8	10.8
	MO3	6.2	78.7	3.3	11.9
	UM2	24.4	56.8	7.5	11.3
	UO2	15.1	61.6	11.0	12.2
Whole sediments	KI3	45.4	48.6	2.4	3.6
	KO1	3.9	88.4	6.0	1.7
	MI2	30.2	50.7	5.7	13.5
	MM4	6.5	76.4	4.3	12.8
	MO3	3.3	72.8	8.0	15.9
	UM2	33.5	47.4	10.1	9.0
	UO2	20.1	54.1	18.2	7.6

Table E.4 Distribution of iron (Fe) under the four binding sites in different particle size fractions (Laboratory replicates, n = 2)

Particle size	Site	Metal concentration (%)			
		F1	F2	F3	F4
Less than 63 $\mu\text{m}$ size	KI3	1.9	13.1	1.0	84.0
	KO1	0.8	10.5	0.7	88.0
	MI2	2.1	39.2	15.7	43.1
	MM4	0.0	46.5	1.3	52.1
	MO3	3.8	28.8	4.5	62.9
	UM2	2.0	17.5	7.8	72.7
	UO2	2.1	20.9	8.0	69.0
Greater than 63 $\mu\text{m}$ size	KI3	0.2	2.59	0.1	97.1
	KO1	0.4	16.5	1.6	81.5
	MI2	1.6	46.5	8.7	43.2
	MM4	0.1	53.0	2.9	44.0
	MO3	7.5	51.0	3.3	38.2
	UM2	2.8	11.5	7.2	78.6
	UO2	3.6	19.5	4.9	72.0
Whole sediments	KI3	3.0	6.5	1.3	89.2
	KO1	1.6	11.3	1.7	85.5
	MI2	2.7	43.5	13.1	40.7
	MM4	0.1	45.6	2.8	51.6
	MO3	9.4	31.8	6.2	52.7
	UM2	3.6	12.0	8.4	76.0
	UO2	3.5	17.0	9.0	70.6

Table E.5 Distribution of Manganese (Mn) under the four binding sites in different particle size fractions (Laboratory replicates, n = 2)

Particle size	Site	Metal concentration (%)			
		F1	F2	F3	F4
Less than 63 $\mu\text{m}$ size	KI3	74.9	18.7	1.7	4.7
	KO1	64.3	23.8	2.3	9.5
	MI2	88.5	9.8	0.9	0.8
	MM4	6.0	92.8	0.8	0.4
	MO3	86.8	9.3	1.2	2.7
	UM2	38.7	49.9	0.9	10.6
	UO2	53.4	39.0	0.8	6.8
Greater than 63 $\mu\text{m}$ size	KI3	61.9	28.9	5.0	4.2
	KO1	20.0	71.4	5.0	3.7
	MI2	82.0	16.4	0.6	1.0
	MM4	5.1	94.4	0.3	0.2
	MO3	84.9	13.3	0.6	1.2
	UM2	39.8	49.2	0.8	10.2
	UO2	48.1	43.8	0.7	7.4
Whole sediments	KI3	79.7	14.9	2.6	2.8
	KO1	46.4	38.5	10.9	4.2
	MI2	91.2	7.9	0.5	0.5
	MM4	6.7	92.4	0.6	0.3
	MO3	93.6	4.9	0.5	1.1
	UM2	45.0	41.7	1.1	12.2
	UO2	59.4	33.7	0.7	6.2

**Appendix F Risk assessment code of selected metals from Zambian polluted wetland sediments**

Table F.1 Percentage acid-soluble fraction in total metal concentration, (%) in different particle-size fractions of the studied sediments

Particle size fraction	Site	Co	Cu	Pb	Fe	Mn
Fraction less than 63 µm size fraction	KI3	78.4	30.1	51.0	2.1	83.4
	KO1	76.0	39.8	37.9	1.0	71.4
	MI2	67.3	55.3	6.3	2.6	94.8
	MM4	0.8	36.4	0.0	0.1	7.78
	MO3	63.2	48.9	4.8	4.4	98.0
	UM2	36.7	50.0	31.4	2.5	51.1
	UO2	52.6	42.3	20.7	2.5	70.2
Fraction greater than 63 µm size fraction	KI3	89.1	18.3	49.8	0.1	63.0
	KO1	76.5	23.4	20.6	0.5	22.9
	MI2	82.7	41.1	3.05	2.0	68.4
	MM4	1.1	30.0	0.3	0.1	5.6
	MO3	82.6	29.2	7.4	7.9	76.8
	UM2	34.9	21.6	24.9	3.6	41.8
	UO2	60.3	16.9	16.4	4.1	48.1
Whole sediments fraction	KI3	95.8	9.1	63.3	3.6	94.6
	KO1	98.2	17.7	3.9	2.1	69.2
	MI2	97.6	83.8	52.3	3.6	81.3
	MM4	1.4	43.9	8.3	0.1	8.4
	MO3	67.5	53.8	4.2	11.8	86.5
	UM2	35.5	40.3	39.4	4.8	56.7
	UO2	57.4	28.7	23.2	4.1	72.4